The sediment routing systems of Northern South America since 250 M

Flora Bajolet, Dominique Chardon, Delphine Rouby, Massimo Dall'Asta, Artiom Loparev, Renaud Couëffé, Jean-Yves Roig

The sediment routing systems of Northern South America since 250 Ma

Flora Bajolet[a, b], Dominique Chardon[a]*, Delphine Rouby[a], Massimo Dall'Asta[c], Artiom Loparev[a], Renaud Couëffe[b], Jean-Yves Roig[b]

a - GET, Université de Toulouse, CNRS, IRD, CNES, F-31400 France

b - BRGM, BP 36009, F-45060 Orléans, France

c - TotalEnergies, Centre Scientifique et Technique Jean Féger, Avenue Larribau, 64018 Pau Cédex, France

Submitted to ***Earth-Science Reviews*** *1rst February 2022*

Revised 17 June 2022 (Manuscript EARTH-D-22-00074R1)

Revised 20 July 2022 (Manuscript EARTH-D-22-00074R2)

* Corresponding author

Email: dominique.chardon@ird.fr

proto-Andean marginal basins, the Central Atlantic rifts/rifted margin basins and the Saharan cratonic basin. After ca. 125 Ma, a cratonic regime of mixed erosion/deposition established and maintained until the onset of the Andean orogeny at ca. 85 Ma. During this period, sediment routes from eroding cratonic domains to the proto-Andean margin basins were episodically closed by inherited Paleozoic structures (i.e., “arches”), whilst sediment fluxes to cratonic or rifted margin basins were partitioned by Atlantic rift shoulders / marginal upwarps of evolving amplitude that formed transient continental divides. After ca. 85 Ma, an Andes-dominated regime installed, in which Andean retro-foreland basins became the main sinks for orogenic sediment fluxes, while exchanges with cratonic basins were controlled by the topographic expression of foreland basins forebulges. Under that regime, cratonic domains mainly acted as by-pass zones for clastic sediments, and their extensive Paleogene and Lower Neogene lateritic covers argue for limited clastic exports from areas exposed to erosion. Very-long wavelength (x 1000 km) asthenospheric support, long-wavelength (x 100 km) lithospheric-scale deformation / vertical movements and climate-controlled erosion processes interacted to regulate cratonic sediment source-to-sink regimes of northern South America since 250 Ma.

Keywords

Source-to-sink; Paleogeography; Andes; Atlantic rifted margin; Intracratonic basin

1. Introduction

The northern part of the South American continent is surrounded by contrasted geodynamic boundary conditions that have evolved through geological time. Its western (Andean) active margin must have recorded subduction since at least the Neoproterozoic (e.g., Schwartz et al., 2008; Capaldi et al., 2021), as implied by global paleo-kinematic

reconstructions (Torsvick and Cocks, 2013; Fig. 1). This active margin evolved as a paired arc / back-arc system until the onset of the Andean cordilleran orogeny in the latest Cretaceous (e.g., Martinod et al., 2020 for a recent review; Fig. 1). To the north, the Atlantic rifted margin of the continent first formed in the Late Jurassic as a consequence of the rifting of the Central Atlantic Ocean (e.g., Labails et al., 2010) (Fig. 1). The remaining Atlantic margins of the continent formed during northward propagation of the South Atlantic Ocean rift in the Early Cretaceous, leading eventually to the formation of its northeastern rifted margin by oblique (transtensional) opening of the Equatorial Atlantic Ocean between 5°S and 5°N (e.g., Heine et al., 2013; Moulin et al., 2010; Fig. 1). Since the early Cenozoic, the northern (Jurassic) rifted margin of the continent has been undergoing dextral transcurrent tectonics accompanying eastward retreat of the Caribbean subduction zone (e.g., Pindell, 1985; Pindell and Kennan, 2009).

These evolving tectonic boundary conditions have resulted in continental deformation and/or vertical movements even far inside the wide cratonic domain of northern South America (e.g., Bicudo et al., 2020; Eakin et al., 2014; Flament et al., 2015; Sacek, 2014). Such movements must have exerted a first-order composite forcing on the sediment routing system that is to say, how sediments were produced, transported, stored on the continent and ultimately delivered to the ocean at its margins. Of particular interest is, for instance, the way sediment fluxes were partitioned between the Pacific or Atlantic sides of the continent, the proportion of cratonic or orogenic sources in those fluxes and whether, where and when sediments were recycled / stored on the cratonic domain.

Source-to-sink and provenance studies of northern South America have mainly addressed the far-field effects of Andean mountain building processes on the cratonic domain (e.g., Cooper et al., 1995; Horton, 2018; Roddaz et al., 2006, 2010). Such studies focused on the Andean retro-foreland basins at the western fringe of the cratonic domain, with an

emphasis on the connection between the retro-foreland basins and the Atlantic rifted margins by the establishment of the modern course of the Amazon River across the continent in the Late Miocene (10-6 Ma; Hoorn et al., 2010, 2017; Mapes et al., 2007). Before that recent drainage rearrangement, uncertainties remain on the evolving configuration of the continent-wide sediment routing systems. Of particular interest are the wide cratonic surfaces exposing basement terrains, which were transiently/repeatedly buried under platform sedimentary rocks beyond today's limits of cratonic sedimentary basins (e.g., Ye et al; 2017). How these surfaces fed proto-Andean active margin basins, cratonic sedimentary basins and rifted continental margins through time is also crucial for our understanding of the length- and time-scales of continent-wide sediment routing systems.

Our study aims at characterizing the responses of the sediment routing systems to the evolving geodynamic forcing at the scale of northern South America with an emphasis on the distribution of source, transit and sink areas, mainly before establishment of the modern Amazon River drainage across the continent. To do this, we produced continent-wide paleo-geological maps for 10 key time periods since the Triassic. Those maps compile the available geological literature and integrate (i) palinspastic/kinematic reconstructions of oceanic and continental landmasses, (ii) major active structural features and magmatic occurrences, (iii) areas of sediment deposition with information on their depositional environments, as well as (iv) constraints on exhumation/burial derived from available thermochronological data. They provide an integrative evolutive framework for the sediment routing systems of cratonic northern South America under the combined influence of active margin / Andean tectonics, Atlantic rifting events and their aftermaths and mantle-driven epeirogeny.

2. Geological outline

The cratonic core of Northern South America is constituted by the Paleo- to Mid-Proterozoic Amazonian shield, comprising the Guiana shield to the north and the Guaporé shield to the south. The two shields are separated by the EW trending Amazonas-Solimões cratonic basin complex. The Amazonian shield is bounded to the west and to the northwest by the Andean orogenic system and to the north and east by the Atlantic rifted margins (Fig. 1a). The Panafrican (i.e., late Neoproterozoic) Braziliano orogen suturing the Amazonian Shield and the Sao Fransisco craton is partially covered by the Parnaíba cratonic basin (Fig. 1b). The Amazonas-Solimões cratonic basin complex initiated as a late Proterozoic-Paleozoic rift that was later inverted to form the Purus arch now separating the Amazonas basin from the Solimões basin (Mosmann et al., 1986; Nuns and Aires, 1984; Fig. 2a). Continuous thermal sag since the Paleozoic allowed those basins to be filled with up to 5 km of sedimentary rocks (Fig. 2a). Regional-scale late Paleozoic to Jurassic wrench tectonics (i.e., the "Jurua orogeny") induced transpression of the Amazonas-Solimões basin complex, which would have set its modern E-W elongate shape (Szatmari, 1983; Mosmann et al., 1986; Fig. 1).

The proto-Andean active margin underwent a protracted history of subduction and arc magmatism since at least the early Paleozoic (e.g., Schwartz et al., 2008; Capaldi et al., 2021). The western termination of the late Paleozoic Variscan collisional orogen, now preserved in the eastern and southern United States (Appalachian - Ouachita orogen) and Mexico, abutted the proto-Andean active margin at a right angle. During the Paleozoic, the proto-Andean active margin underwent alternating phases of fore- and back-arc basins opening, closure and accretion that are partly recorded in modern Andean retro-foreland basins (Mathalone and Montoya, 1995). The hinterland of the active margin underwent Paleozoic transgression-regression cycles that deposited fluvio-deltaic to deep marine sequences now preserved in intracratonic basins (Mosmann et al., 1986). The Meso-Cenozoic sedimentary rocks thickness in intracratonic basins is negligible compared to that in Proto-Andean marginal basins and

Andean retro-foreland basins (Figs. 1 and 2) but have a continental extent. Most Mesozoic sedimentary rocks (mostly Cretaceous) are preserved in rifted basins (rifted margins and intracontinental rifts) and Andean retro-foreland basins, whereas Cenozoic sedimentary rocks are mainly preserved in Andean retro-foreland basins (Fig. 2).

The CAMP (Central Atlantic Magmatic Province) magmatic episode, that occurred during a short period of about 5 Myr at the Triassic-Jurassic boundary, left an important imprint in northern South America. Extensive tholeiitic magmatism spread over more than 12 10^6 km^2 and lava flows of the Amazonas-Solimões and Parnaíba basins alone represent about 2.4 10^5 km^3 (Wanderley-Filho et al., 2005). CAMP magmatism is assumed to originate from either a single mantle plume (May, 1971; Morgan, 1983), or a superplume that triggered Pangea dispersal (e.g., Romanowicz and Gung, 2002; Condie, 2004). The latter hypothesis is still contentious (e.g., Peace et al., 2020). But the location of many hotspots, Large Igneous Provinces (LIP) and kimberlites over Pangea at 200 Ma however fits the surface projection of a mantle Large Low Shear Velocity Province (LLSVP; Ruiz-Martinez et al., 2012) rooted in the core-mantle boundary and stable since at least 300 Ma (Burke et al., 2008). That LLSVP represents a mature mantle thermal / compositional instability that could have indeed produced the CAMP and triggered Pangea breakup (Burke et al., 2008).

3. Methods

We compiled the paleo-geological maps from published studies. We included (1) sedimentation areas and their depositional environments, (2) sediment transport routes based on paleocurrent measurements and provenance studies from detrital geochronology and heavy minerals associations, (3) magmatic occurrences, (4) active faults, (5) local thermal histories from low-temperature thermochronology (heating or cooling) and (6) areas that underwent Cenozoic extensive lateritic weathering and preserve bauxites / laterites in their landscape

(Fig. 3a; Table 1). The geodynamic context, including plate boundary configurations and kinematics, was compiled mostly from published models (e.g., Matthews et al., 2016; Moulin et al., 2010; Pindell and Kennan, 2009). We used the palinspatic configuration at the end of the considered time period of each map, in a fixed South America reference frame. Mentioned geographic coordinates refer to that reference frame.

We compiled a Late Permian map to illustrate the pre-Pangea break-up configuration (Fig. 5), seven Mesozoic maps corresponding to the main phases of the Atlantic margins stratigraphy in order to facilitate continent-ocean source-to-sink interpretation (Figs. 6 to 11), as well as two Cenozoic maps (a Paleogene stage corresponding to a continent-wide sedimentary hiatus and the Middle Miocene configuration i.e., just before the establishment of the modern Amazon drainage; Figs. 12 and 13). Time intervals between paleo-geologic maps are generally of the order of 10 Ma.

Following Ye et al. (2017), we mapped sedimentation (sink) areas on the basis of the area of today's preserved deposits and, beyond, the minimal areal extent of the considered beds at the time of deposition (respectively dark and light colored on Figs. 4 to 13). This minimal areal extent of deposition is estimated from the mean regional slopes of cratonic and rifted margin basins and the mean denudation rates given by thermochronology (ca. 10 m/My; following the method of Ye et al., 2017).

The paleo-geological maps were mostly compiled from published data and interpretations (e.g., geological contours, logs and cross-sections, structural data, provenance studies) taken from published geological maps, charts and published paleogeographic maps that we harmonized and updated with local / regional studies. These documents, that allowed to map more than 90% of the map area, are listed in Table 1 where the specific time slice(s), region(s) and topic(s) they have been used for are indicated. In addition, reconstructions of the Atlantic margin of South America were mostly derived from Loparev et al. (2021) (see Fig.

S1, supplementary material, for the position of the cross sections) as well as the paleo-geological maps of Ye et al. (2017) for northwestern Africa and its Atlantic margins, complemented by 17 studies (Table 1). We locally further validated our mapping at onshore wells where available (Fig. S1, supplementary material).

In the following comments of the maps, authors are cited for specific information and interpretations that may not be explicitly reported on the maps. Figure 3b shows the main localities and geological elements referred to in the text, some specific elements being also indicated on the paleomaps of Figures 4 to 13.

4. Paleo-geological maps

4.1. Permian (270-250 Ma): continental record of erosion of the Appalachian orogen (Fig. 4; Table 1)

In the Middle and Late Permian, Pangea recorded the latest stages of its assembly along the collision of Western Gondwana (Africa, South America) with Laurentia (North America in the present case). The late Paleozoic (i.e., Variscan) Mauritanides were being eroded and feeding North American molasse basins. Eastward subduction beneath the western American proto-Andean margin is attested to by magmatic remnants currently scattered in Mexico and the northern Andes. The aridification of the continental interior and the general marine regression allowed for the deposition of evaporites and red beds in most of the basins. The two main depocenters were the Amazonas-Parnaíba basin and the Saharan basin in West Africa, while southeastern Brazil intracontinental rifts (Borborema province) recorded coastal/deltaic sedimentation. Those deposits were probably connected to the deltaic/shallow marine Lower Permian sequences of Congo (Linol et al., 2015a, 2015b, 2016) and/or the Paraná basin, south of the study area (Milani et al., 2007; Simões et al., 2016). Coastal basins of the western active margin south of the modern equator recorded shallow marine to

lacustrine sedimentation and volcanism, marking the initiation of back-arc extension. Outside the proto-Andean marginal domain, a regional unconformity sealing the Permian sedimentary sequences is generally interpreted as the signature of latest Appalachian/Variscan regional uplift movements (Craddock et al., 2017; Hamlin, 2009).

In terms of sediment routing systems, our mapping suggests that the main sources of detrital sediments for the intracontinental basins were the late Paleozoic orogens (Mauritanides-Appalachians-Ouachita) and more generally the Gondwana crust. Sediments were either transiently stored in cratonic basins and/or exported to the southern margin of the Paleo-Tethys Ocean (to the NE of the mapped area), the Congo/Paraná basins (to the SE of the mapped area) or the proto-Andean margin basins.

4.2. Triassic-Jurassic (235-190 Ma): CAMP, Central Atlantic rifting and very long wavelength cratonic uplift and denudation (Fig. 5; Table 1)

Central Atlantic rifting initiated at the Triassic-Jurassic boundary (de Matos, 1999), contemporaneously with CAMP magmatism (e.g., Marzoli, 1999). Andesitic to tholeiitic (mostly) magmas emplaced as lava flows, sills and dikes over a very large area that comprises most of northern South America. Numerous sills, up to 1 km-thick, intruded the Amazonas-Solimões basin complex. Dikes, striking mostly SE, intruded the northeastern Amazonian craton and the West African craton. Lava flows and kimberlites are also reported in various cratonic basins between 0 and 15°S.

Central Atlantic rifting initiated between North and South America with the opening of the Texas basin and individualization of the Yucatan block. The Western active margin of America was undergoing active subduction, magmatism and back-arc extension. The Amazonian craton was therefore fringed to the east, north and northeast by extensional basin systems. Arc magmatism lasted until the end of the Jurassic in the northern Andes (Colombia)

while the Lower-Middle Triassic volcano-sedimentary sequences of the proto-Andean margin were drowned under a carbonate platform in the Late Triassic-Early Jurassic. Fluvio-lacustrine to transitional environments in the Acre basin marked the transition between the proto-Andean margin domain and the continental cratonic domain under the CAMP influence.

To summarize, the Triassic-Jurassic period was dominated by widespread CAMP magmatism as well as nonmarine deposits in dominantly arid environments around the Amazonian shield. The unconformity sealing the Triassic sequences over the South American and African cratonic areas (e.g., Guiraud et al., 2005) marks a general sedimentary hiatus. Paleozoic cratonic basins, and, to a lesser extent, Triassic deposits, must have therefore shifted from sinks to sources at this time, feeding the Central Atlantic rifts and the proto-Andean back-arc basins.

4.3. Valanginian (140-133 Ma): Maintained cratonic denudation and upwarping (Fig. 6; Table 1)

We did not compile any map for most of the Jurassic (190-145Ma) because it was a period of sedimentary hiatus in cratonic environments. A regional unconformity seals Jurassic series in cratonic and most marginal basins (Milani et al., 2007). In the Early Valanginian (140 Ma), sedimentation in the proto-Andean margin still recorded back-arc extension. Several volcanic arcs were active and a forearc basin formed. Stratigraphic studies have shown that at least one major west-facing normal fault system was active during the Mesozoic at the eastern boundary of the back-arc domain (i.e., the Chonta fault; Scherrenberg et al., 2012). Positive inversion of such faults during Andean orogeny contributed to the growth of major structural highs (i.e., “arches”) such as the Marañon “anticline” (e.g., Scherrenberg et al., 2014).

The rift-drift transition in the Central Atlantic and Gulf of Mexico formed the northern rifted margin of South America in the Early/Middle Jurassic (Ismael, 2014; Matthews et al., 2016; Seton et al., 2012). Little information is available for that margin because of its inversion in the Cenozoic. Rifting was active at the western tip of the future equatorial Atlantic Ocean, in the Demerara plateau and Guinea Plateau areas, as well as farther south in the Tacutu graben. Nonmarine deposits in the Marajo basin suggest a diffuse thermal extension in the area ("sag"; Zalán and Matsuda, 2007). South Atlantic rifting, propagating northward, reached the southeasternmost part of the mapped area. Nonmarine deposits accumulated in the associated grabens as well as over a wide surrounding area (in Africa and South America) locally drained southward.

To the northeast, the Saharan cratonic basin grew laterally under nonmarine depositional environments. The remaining cratonic domains in Africa and South America underwent erosion, consistently with cooling thermochronology data compatible with exhumation in these domains and kimberlite magmatism suggesting uplift. The African surface configuration suggests the occurrence of an upwarp between the future Atlantic margin and the Saharan basin. A conjugate erosional upwarp exhuming the Guiana shield and the Guaporé Shield is also expected. These upwarps appear to be linked to incipient rift propagation at the southeastern tip of the Central Atlantic. They are part of a wider source/bypass dome exposing the Northern South American cratonic domain and the West African craton in between an African interior sink and the proto-Andean margin. This suggests a very long-wavelength deformation control on topography and sediment routing systems driven by mantle support, with essentially the same distribution of source and sink domains since the CAMP period.

4.4. Aptian (120-115 Ma): Equatorial Atlantic rifting and initiation of a cratonic basin (Fig. 7; Table 1)

During the Aptian (120-115 Ma), the Equatorial Atlantic rifting further developed as an oblique en-échelon rift system while the Marajo and Takutu grabens underwent further extension. All the rift basins received nonmarine deposits, except in the previously rifted Guinea and Demerara plateau basins that were already under marine conditions. Transpressive inversion structures (E-W folds and oblique-reverse faults) developed along the strike-slip corridor between the Demerara and Guinea plateaus as a consequence of a southward shift in the rotation pole of Africa. This inversion also formed NE-trending structural arches bounding the Marajo and Parnaíba basins.

The northern rifted margin underwent low-amplitude transgressions bringing clastic deposits with minor carbonates fringed by shoreface/deltaic systems A flip in subduction polarity led to the subduction of the Atlantic plate beneath the Pacific plate i.e., the Caribbean subduction, initiating eastward retreat. A transform fault linked the Caribbean subduction to the Andean subduction. At the northernmost tip of the South Atlantic rift system, the continental basins of the Borborema province underwent thermal sag and fluvio-lacustrine sedimentation with a few marine incursions during the Late Aptian-Early Albian. This basin was connected to the African interior via the Benue corridor, which was supplied by SW-flowing African rivers. The S- to SE-directed paleocurrents in the western Borborema basin and the exhumation recorded by thermochronology immediately west of the basin suggest the occurrence of a marginal upwarp bounding the basin to the west. While cratonic basins in Africa remained under nonmarine sedimentation, the Parnaíba basin, isolated by two new structural arches, received non-marine and shallow marine sediments from the Middle Aptian to the Late Albian. Accommodation of fluvio-deltaic and aeolian sedimentation in the San Franciscana basin may be interpreted as a rift infill (e.g., Reis et al., 2017). SW-directed

paleocurrents in the basin could indicate the occurrence of an upwarp between the San Franciscana basin and the South Atlantic rift domain of the Borborema province. Provenance studies indicate that the basement of the Atlantic rift shoulders became a source for the Atlantic rifts of the Borborema province, with an additional contribution of Jurassic and Paleozoic sources (Figueiredo et al., 2016). This suggests that a pre-Cretaceous sedimentary cover was still outcropping in the cratonic domain during the Aptian.

Sedimentation resumed in the Amazonas - Solimões basin complex with the fluvio-lacustrine Alter do Chao Formation. Biostratigraphy indicates that this formation is Aptian to Maastrichtian in age, although continuity of the sequence over the period and across the basin remains debatable (Daemon, 1975; Daemon and Contreiras, 1971; Dino et al., 1999). We therefore used the same contours of preserved deposits of the Alter do Chao Formation for the Aptian to Maastrichtian maps (Figs. 7 to 11). Paleocurrents and provenance studies document a westward flowing drainage in this formation, likely feeding the proto-Andean margin basin(s). This drainage was separated from the short coastal drains flowing toward the Central Atlantic rift system by the Purus Arch that formed the continental divide at the time. The Alter do Chao formation yielded a unique Paleoproterozoic (2.3-2.0 Ga) detrital zircon population (Dantas et al., 2014; Mapes, 2009) that contrasts with the common Silurian-Early Devonian signature in the Amazonas - Solimões basin complex. This could suggest a unique source in the Guiana Shield that mostly comprises Transamazonian (2.3-2.0 Ga) basement. The western boundary of the Amazonas-Solimões basin was formed by the NW-trending Iquitos arch, an inherited basement structure (Moreno-López and Escalona, 2015; Pryer et al., 2009; Sánchez et al., 1999) that repeatedly isolated the complex from the Acre basin during Cretaceous times. The Iquitos Arch was generally flooded during transgressions and emerged during regressions. It was not necessarily repeatedly uplifted, as stratigraphic architectures

suggest that mostly eustasy controlled connections between the Solimões basin and the proto-Andean basins (Da Cruz Cunha et al., 2007; Martínez et al., 1999).

Along the proto-Andean margin, only a few back-arc basins were still active and most entered a thermal sag stage (Mathalone and Montoya, 1995; Sarmiento-Rojas et al., 2006). A normal fault-bounded, large-scale topographic high grew in the Peruvian Andes that will be inverted later, during the Andean orogeny, to become the Marañon anticline. That structure divided the margin into two sub-basins i.e., the West and East Peruvian Troughs. A marine transgression initiated in the West Peruvian Trough, leading to coastal sedimentation passing to nonmarine sedimentation eastward. The Peruvian basins have Precambrian-Paleozoic crystalline basement sources coming mainly from the Amazonian shield, with minor contributions of Paleozoic to Early Cretaceous sedimentary rocks (Horton, 2018; George et al., 2019). They were probably fed by scattered local highs inherited from Jurassic-Early Cretaceous back-arc rifting and arc magmatism. Along the northern portion of the active margin (between 2°N and 2°S), shoreface and fluvial deposits have cratonic basement and Paleozoic sedimentary sources with a minor input from local igneous rocks (Gutiérrez et al., 2019; Vallejo et al., 2017; White et al., 1995). The Amazonian craton and Paleozoic sedimentary rocks outcropping today east of the basin are the most likely candidates for those Aptian sources. Along the northwestern margin of the continent, shallow marine sequences were sourced from cratonic basement and Jurassic volcano-sedimentary rocks eroded from local highs (Horton et al., 2015). The Jurassic signature vanishes in the eastern part of the basin where Precambrian and Paleozoic igneous and sedimentary sources dominate until the early Cenozoic (Horton et al., 2010). The Aptian sedimentary sequences overlay series derived from local sources. A regional drainage reorganization is therefore suspected to explain the onset of dominant cratonic fluxes to the western margin of South America.

In terms of sediment routing systems, Aptian paleogeography was characterized by the renewal of sedimentation over cratonic South America, which was compartmentalized by marginal upwarps and intracontinental structural highs. Toward the future Equatorial Atlantic fringe of the continent, this pattern seems to have been influenced by the segmentation of the Equatorial Atlantic rift system into oblique and transform portions (e.g., Loparev et al., 2021). Cratonic areas were also fed with clastic sediments. The proto-Andean marginal basins in their thermal sag phase. At the same time, south of the equator, proto-Andean basins were being filled with nonmarine sequences.

4.5. Albian (107-100 Ma): Post-rift of the Equatorial Atlantic and marine transgression (Fig. 8; Table 1)

The first order Albian paleogeography remained similar to that of the preceding period until the end of the Mesozoic in terms of source-sink/by-pass areas and tectonic boundary conditions (Fig. 7). In the Albian, the separation from Africa is achieved by seafloor accretion in the Equatorial Atlantic, except in the Guinea-Liberia basin resting upon hyperextended continental crust (Ye et al., 2017). The Takutu graben, which has reached its sag phase, underwent nonmarine sedimentation. The equatorial Atlantic margins of South America have reached their drift stage. A vast lagoon developed in the Parnaíba basin, collecting sediments from the surrounding areas, including the Borborema province and the Barremian-Lower Albian deposits of the southern San Franciscana basin (see Fig; 7). Thermochronology indicates that the southeasternmost part of the map underwent exhumation, and probably uplift, and may also have been a potential source for the Paranaíba basin.

North of the equator, local intraplate tholeitic to alkaline magmatism activity took place in back-arc rifts, possibly as a result of a late extensional reactivation (Vásquez and Altenberger, 2005) or negative inversion (Barragán et al., 2005). In the transform zone linking

the Carribean and Andean subductions, a dextral pull apart basin developed that received thick volcaniclastic series. Moderate folding of these rocks shortly after their deposition is interpreted as due to an increase in the convergence rate across the future Andes (Mochica phase; Jaillard, 1994; Pfiffner and Gonzales, 2013; Soler and Bonhomme, 1990). Farther south along the active margin of South America, a transgression led to the deposition of a wide (>400 km) strip of shallow marine deposits fringed landward by deltaic/coastal and nonmarine environments. Cratonic sources prevail in proto-Andean margin basin sedimentary rocks (Saylor et al., 2011; Vallejo et al., 2007) while the Iquitos arch - prolonged to the south by the Marañon anticline - acted as a boundary between the cratonic and active margin basins. Therefore, the wide Amazonas-Solimões cratonic basin complex might have been temporarily endorheic during the period because it was also isolated at least intermittently from the Atlantic margin domain by an upwarp. The warm Early Cretaceous climate, especially from Albian to Cenomanian (Tardy and Roquin 1998), likely favored laterization of source/bypass areas and alluvial plains.

In terms of sediment routing systems, the Albian configuration of South America was similar to that of the Aptian, with cratonic regions being the source of clastic sediments for both intracontinental basins and marginal sinks. The equatorial Atlantic margin had reached the drift phase and the rift-related onshore arches were no longer active, allowing a single wide depocenter (i.e., the Parnaíba basin) to collect sediments from surrounding areas. On the proto-Andean margin, global sea-level rise allowed for wide shallow marine systems to develop, contemporaneously with arc magmatism, while northeastward slab roll-back proceeded at the northwestern edge of the continent.

4.6. Cenomanian 97-93 Ma: Maximum marine flooding and continental-scale floodplain (Fig. 9; Table 1)

The Cenomanian global sea-level maximum pushed the coastline farther inland compared to the Albian. The marine incursion into the Marajo graben allowed for a wide embayment to form in the Parnaíba basin. In the Amazonas basin, the sandstones of the Alter do Chao formation recorded shoreface/foreshore/deltaic environments with bi-directional currents. Although not precisely dated, those beds most likely represent the Cenomanian eustatic peak. Along the active western margin of the continent, shallow marine sedimentation extended farther inland and deep marine environments were recorded north of the Guiana shield and farther west (Maracaibo region; La Luna Fm.). The Solimões basin was then connected to both the proto-Andean and Atlantic margins and drainages may have flowed both ways (Da Cruz Cunha, 2007). Drainage divides south and north of the Solimões basin may not be precisely mapped. However, given the paleocurrent directions and documented paleo-drainage patterns, the Amazonas embayment could logically only be fed by proximal cratonic sources (i.e., eastern parts of the Guiana and Guaporé Shields). Cratonic sources still fed the proto-Andean marginal basins at least north of the Solimões basin (Horton, 2018; Saylor et al., 2011).

In terms of sediment routing systems, the Cenomanian paleogeography was thus dominated by transgressions allowing marine sedimentation far inland whilst erosion of cratonic domains fed all the basins.

4.7. Santonian (86-84 Ma): Intracratonic sedimentation and onset of Andean orogeny (Fig. 10; Table 1)

With the Santonian lowering of the global sea-level, nonmarine sedimentation resumed with fluvial, lacustrine and eolian deposits in most of cratonic basins (Amazonas-Solimões, Parecis, San Fransiscana). The deposition of a widespread cover over most of the Guaporé craton is not precluded. The Parnaíba embayment became exposed and underwent

erosion/by-pass. Paleocurrents suggest at least three main drainage systems on the cratonic domain: (i) a narrow (<200 km) Atlantic coastal drainage that reached far inland (>1500 km) in the southeastern part of the study area, (ii) a vast drainage towards the Amazonas - Solimões alluvial plain and potentially (iii) a southward drainage in the Parecis lowland. Cratonic basins were connected to the proto-Andean region as shown by the continuity of deposits across the Iquitos arch. Nevertheless, the arch localized the deltaic/nonmarine transition and was therefore still active.

Proto-Andean marginal basins recorded shallow marine sedimentation. The increase in convergence rate or in subduction coupling produced several emergent compressive structures along the active margin (Jaillard, 1994, Jaillard et al., 2009). The southern part of the active margin recorded voluminous arc magmatism coeval with the main phase of Galapagos hot-spot magmatism. Subduction of the Farallon plate beneath the Caribbean plate initiated, forming the Central America arc. The terranes dragged northeastward by Caribbean subduction roll-back along the transform domain were sequentially accreted onto the northern Andean margin (e.g., George et al., 2021, Jaillard, 2022, and references therein).

In terms of sediment routing systems, the Santonian saw most cratonic domains undergoing sedimentation. Only two erosional areas sourced sediments. The Guiana shield exported sediments towards the Atlantic margins, the Pacific margin and the Amazonas-Solimões basin complex, whereas southeastern Brazil (i.e., East of 55°W), still undergoing uplift, mainly fed the Atlantic margin and the San Franciscana basin.

4.8. Maastrichtian (72-66 Ma): Growth of the Andean retro-foreland basins (Fig. 11; Table 1)

The Maastrichtian cratonic paleogeography remained similar to that of the Santonian except for the cessation of sedimentation in the easternmost Parecis basin. Deltaic systems

developed along the entire Atlantic rifted margin from the Marajo graben to the northwestern tip of the continent.

The slab roll-back dragged the Caribbean plate northward so that its northern edge has reached northwestern South America while magmatism remained active all around the plate. Along the western active margin, island arc and back-arc basins closed while magmatic arc accretion initiated between Quito and Piura. East-vergent thrust tectonics led to more conspicuous exhumation of Andean basins SE of the transform domain (Bayona et al., 2008; Cooper et al., 1995; Villamil, 1999). Sea retreat was enhanced by tectonically-driven topographic growth. Clastic sediments derived from the young Andean topography filled early retro-foreland basins. North of the equator, paleoenvironments of the proto-Andean domain were shallow marine with mixed cratonic/Andean sources while, farther south, they evolved to transitional /nonmarine with mainly Andean sources (Louterbach et al., 2018; Saylor et al., 2011; Vallejo et al., 2017, 2019). The continuity of deposits across the Acre basin suggests a connection between the retro-foreland and cratonic basins. However, the lack of Cretaceous deposits at some locations near the Iquitos arch and the unconformity at the top of the sequence suggest only partial/intermittent connections (Feijó and Souza, 1994; Martínez et al., 1999). The Iquitos arch may have acted as the forebulge for the young retro-foreland basin as it has during Cenozoic times (Roddaz et al., 2006). Thermochronology data are consistent with exhumation in southeastern Brazil and Eastern Guaporé Shield, as well as in the eastern Guiana Shield.

In terms of sediment routing systems, the Maastrichtian shows major sea retreat, growth of the Andes by thrusting and the onset of retro-foreland basin sedimentation, which was mainly sourced by early Andean internal tectonic relief, and shifting from marine to nonmarine environments. Intracratonic sources and sinks remained similar to those of the Santonian, with continuing uplift and exhumation of southeastern Brazil.

4.9. Lutetian-Bartonian (48-38 Ma): Weathering cratonic regime and ongoing Andean sediment supply (Fig. 12; Table 1)

In the Mid-Eocene, Caribbean slab rollback had built orogenic topography in the northernmost segment of the Andes, along a transpressive deformation belt (e.g., Mann et al., 2006). The Caribbean plate roll-back started dragging the Central America trench (subduction of Farallon plate beneath Caribbean plate) and related arcs northeastward. A continental magmatic arc developed in the Andes between the equator and 8°N. In that portion of the Andes, most terranes have reached their modern positions, building cordilleras and intermontane domains. In most retro-foreland and cratonic basins, a major unconformity seals the Cretaceous deposits. In the retro-foreland basins, that unconformity was classically interpreted as the signature of a Late Paleocene-Early Eocene "Incaic phase" of Andean building (e.g., Jaillard, 1994). More recently, the unconformity was interpreted as reflecting a period of orogenic quiescence instead (e.g., Horton, 2018, 2022).

The upper Andean piedmont received mostly nonmarine clastic sediments. Nevertheless, sporadic marine incursions occurred, either via a corridor crossing the Andes (around 3°S; Louterbach et al., 2014) or via the long NNE-trending Orenoco river estuary, whose mouth was located near Maracaibo at the time. Tectonic topographic building along most of the orogen led to the mobilization of Andean Mesozoic volcano-sedimentary and basement sources for sedimentation in the retro-foreland basins (Caballero et al., 2013; Silva et al., 2013; Horton, 2018).

Outside the Andean foreland basin, all the continental surfaces underwent very slow erosion or bypass, without criteria to assess the main drainage configuration. Cratonic domains therefore show no preservation, although a residual Solimões alluvial or lacustrine basin may have maintained. The Cenozoic greenhouse warm and wet climate favored

continental chemical weathering over mechanical erosion, resulting in subdued clastic fluxes to the sediment routing system. The considered period (Lutetian-Bartonian; 48-38 Ma) is that of an extensive bauxitic lateritic weathering in northern South America, Africa and India (Prasad, 1983; Tardy and Roquin, 1998).

In terms of sediment routing systems, during the Middle Eocene, all cratonic domains underwent very slow erosion or by-pass and extensive lateritic weathering due to peak greenhouse climate. Active erosion in the Andes reworked sedimentary sources of various ages to feed the retro-foreland basins.

4.10. Langhian-Serravalian (16-12 Ma): Growth of the Andean retro-foreland basin at the expense of the cratonic domain (Fig. 13; Table 1)

By the Middle Miocene, nonmarine sedimentation had resumed in the Solimões and eastern Parecis basins. The mid-Miocene thermal optimum favored continued / renewed production of laterites and the preservation of the Paleogene lateritic covers. In the Amazonas and Parnaíba basins, several lateritic horizons in Miocene series intersperse with fluvial deposits (Abinader, 2008; Rossetti, 2001; Rosseti and Netto, 2006). This is consistent with a low denudation regime over most of the exposed land and limited clastic sediment exports from the cratonic domain. In the Amazonas basin, southeastward paleocurrents suggest a drainage divide between the Amazonas and Solimões basins localized on the Purus arch.

Renewed uplift during the Neogene finalized the modern architecture of the Andes and its retro-foreland, alongside the eastward propagation of the deformation front (Bayonna et al., 2008; Eude et al., 2015; Pfiffner and Gonzales, 2013). The Andes were the major source of sediments for all retro-foreland basins, which received recycled Paleogene Andean strata in addition to Mesozoic sources (Caballero et al., 2013; Moreno et al., 2020; Roddaz et al., 2006). The orographic barrier of the northern Andes prevented the retro-foreland basins

drainage to flow directly northward. The main drainage axis (Orinoco River) progressively shifted eastward from the Eocene onward (Escalona and Mann, 2011), accompanying Caribbean trench retreat. Arc collision and transpression went on along the northeastern active margin as Caribbean slab roll-back proceeded. A southward marine transgression in the northern retro-foreland basin reached about 3°N and triggered episodic marine deposition. A mega-wetland recording lacustrine/deltaic/marine environments developed over a large area connecting the retro-foreland and the cratonic basins despite the Iquitos forebulge (i.e., the "Pebas sea").

The Galapagos ridge, formed at ca 20 Ma, separated the Cocos and Nazca plates and subducted beneath the Panama arc. Various blocks accreted to form Central America, which almost reached its present-day location while island arc volcanism initiated at the eastern edge of the Caribbean plate. Active continental arc volcanism along most of the Andes reflected subduction and Andean growth.

In terms of sediment routing systems, the Middle Miocene showed continued lateritic weathering of the cratonic domain undergoing very slow erosion and by-pass. A large Northern Andean retro-foreland sink received repeated marine incursions from the Orinoco River valley (the Pebas mega-wetland). Andean mountain building, following the last plate reorganization in the Pacific domain, increased sediment supply to the retro-foreland basins for which it was the main contributor.

Afterwards, during the Late Miocene, the establishment of the modern course of the Amazon River across the continent connected the Andean retro-foreland and the Atlantic margin basins (at ca. 10-6 Ma; Hoorn et al., 2010). Indeed, the peak in topographic growth in the Andes increased sedimentary supply in the retro-foreland basins that eventually became overfilled (Sacek, 2014). In response, retro-foreland drainage system grew eastward into the

Amazonas basin, flooding the Purus Arch and eventually connected to a coastal river valley to form the modern Amazon River.

5. Discussion

The cratonic sediment routing systems evolved between, and under the influence of, the Atlantic rift / rifted margins and the proto-Andean active margin / Andean orogen (Figs. 1 and 14). Within that framework, the main controls on sediment pathways were exerted by (i) the Amazonas-Solimões axis, as a bypass or storage trough, (ii) the Atlantic marginal upwarps, (iii) the structurally controlled arches between intracratonic and proto-Andean margin basins and (iv) forebulges of the Andean retro-foreland basins (Figs. 1, 2 and 14). These elements of the sediment routing system were also temporarily erosional (source) areas for the adjoining sedimentary basins.

5.1. The Amazonas - Solimões basin complex: a persistent sediment transit route across the continent

The long-lasting Amazonas-Solimões basin complex remained the main connection between the cratonic domain and the Proto-Andean/ Andean domain on the one hand, and the Atlantic rifted margin domain, on the other hand. During Paleozoic times, while shallow marine sedimentation covered large areas of Gondwana, the basin complex formed an elongate sag basin. It remained an E-W trough afterwards, acting as an intermittent drainage axis regulating sediment fluxes across Pangea until the Early Cretaceous. After the onset of equatorial Atlantic rifting and onward, the trough became a corridor between the Andean and Atlantic margin basins, acting alternatively/repeatedly as a pathway, a storage area or locally an erosional source for clastic sediments (Fig. 14). As such, it was the central regulating

element of the continental-scale sediment routing system that collected sediments from cratonic and Andean sources.

The width of the Amazonas-Solimões basin complex must have evolved through time, with sedimentary rocks deposited beyond its current northern and southern margins. Those sedimentary rocks were eroded away and their erosional products may have transited through cratonic domains northward via the Takutu graben to the Atlantic margin (e.g., in the Albian-Aptian; 120-100 Ma; Figs. 7, 8 and 14) and/or southward to the Parecis basin (e.g., in the Santonian and Maastrichtian: 86-66 Ma; Figs. 10, 11, and 14). These sediment fluxes and their age cannot however be assessed precisely because of the lack of Mesozoic or Cenozoic sedimentary remnants on the Guiana and Guaporé Shields.

The maintenance of the Amazonas-Solimões trough over the Meso-Cenozoic can be explained by its structural inheritance as an initial rift structure and/or its Jurassic inversion (i.e., Jurua orogeny). But if the trough actually passively guided the Late Miocene installation of the modern Amazon River course that connected Andean retro-foreland and the Atlantic margin basins, an additional mantle-scale process appears to be required to trigger that drainage reorganization (Shephard et al., 2010). Indeed, the very-large extent/wavelength of the Pebas mega-wetland (Fig. 13) and its persistence during the Middle Miocene despite the Iquitos forebulge was probably due to dynamic (i.e., asthenosphere-driven) subsidence rather than to lithospheric processes (i.e., tectonic faulting, lithosphere flexure; Shephard et al., 2010). At that time, the main N-S axial drainage of the Andean retro-foreland was separated from the cratonic basins by the Purus arch. Sacek (2014) and Shephard et al. (2010) proposed that the peak in Andes exhumation increased the sediment supply to the retro-foreland, pushed the axial drainage eastward, buried the Purus arch and resulted in the migration of the continental divide. Andean sedimentary wedges then prograded eastward and hampered the northward-flowing river drainage toward the Guiana and Guaporé Shields. Ultimately, an

overspilling piedmont drain connected to an Atlantic coastal river via the Amazonas-Solimões trough, resulting in the modern Amazon River drainage. Numerical simulations of Bicudo et al. (2020) coupling an increased piedmont sedimentation, correlative lithosphere flexure and dynamic topography responding to westward subducting slab dynamics under the retro-foreland, suggest that a low amplitude dynamic topography fits better the final volume of Cenozoic sedimentary rocks in the Solimões basin.

5.2. The Triassic to Aptian sedimentary hiatus: evidence for a long-lasting superswell

This sedimentary hiatus suggests a long-lasting (100 Myr), very-long wavelength (>3000 km) control on the sedimentary systems that we interpret as a mantle-supported, eroding topographic superswell (Fig. 14). Mantle dynamics numerical models indeed predict such a domal surface uplift with an amplitude of a few hundred meters to 2 km in response to a hot asthenospheric mantle rise (e.g., Flament et al., 2015; Gurnis et al., 2000). The superswell and correlative erosion must have been sustained by the heat accumulated in the mantle under Pangea by continental insulation following the supercontinent assembly in the latest Paleozoic (e.g., Coltice et al., 2007; Ganne et al., 2016).

Given the great size of the area affected by the sedimentary hiatus and its duration, significant sedimentary fluxes are to be expected towards basins surrounding the superswell (i.e., the Saharan basin, the proto-Andean active margin basins and the northern (Atlantic) margin basins, the Congo basin; Figs. 4 to 6). But a source-to-sink balance would be elusive for several reasons such as (i) the erosion of proto-Andean series during Andean orogeny, (2) the consumption of proto-Andean series and Central Atlantic margin sedimentary rocks by Pacific and Caribbean subductions, (iii) the fact that Central Atlantic margin syn-rift sedimentary sequences may actually be mostly volcanic (e.g., Sapin et al., 2016) and (iv) the

tapping of the Saharan basin sedimentary rocks that were exported northward into the Tethys (Ye et al., 2017).

5.3. Albian and Late Cretaceous marginal upwarps and forebulges: Evolving checkpoints between intracratonic and margin basins

A series of marginal upwarps (or upwarp segments) grew in South America as a consequence of Cretaceous rifting. These upwarps acted mostly as continental divides between the rifted margin basins and the intracratonic basins (Fig. 7). If the Guiana Shield upwarp segment remained a divide until the end of the Cretaceous (Figs. 7 to 11), segments located farther to the SE evolved through time. For instance, the upwarp formed on the Gurupa arch separating the Marajo rift from the Amazonas basin, vanished after the Albian (100 Ma; Figs. 2a, 8 and 9). A drainage divide, potentially related to a shoulder flanking the Parnaíba basin to the south during the Aptian (120-115 Ma; Fig. 7), was flooded in the Albo-Cenomanian (107-93 Ma; Figs. 8 and 9). Pre-Mesozoic structures, acting as arches to the east and the west of the Parnaíba basin, also imprinted the margin drainage pattern in the Aptian (120-115 Ma; Fig. 7). The marginal upwarp documented in the Borborema province during the Cenomanian (97-93 Ma; Fig. 9) was then eroded away in the Santonian (86-84 Ma; Fig. 10).

To summarize, Albian and Late Cretaceous sediment pathways between cratonic North America and its Atlantic margin basins were compartmentalized by a network of marginal upwarps and rift shoulders whose topography evolved through time (Fig. 14). In terms of source-to-sink, this resulted in an evolving drainage pattern and modifications of source areas both for Atlantic margin basins and intracratonic basins.

During the Late Cretaceous, the transit of sediments between the cratonic domain and proto-Andean marginal basins has been modulated by the reactivation of N-S to NE-SW

trending, inherited Paleozoic structures (Albian to Maastrichtian: 107-66 Ma; Figs. 8-11). Between 5°N and the equator, such structures prevented marine transgressions from the Gulf of Mexico/Caribbean domain and sediment transfer to the cratonic domain. Farther south, the Iquitos arch emerged intermittently. During the Early Cretaceous and the Early Late Cretaceous, the arch was a passive barrier that became the forebulge of the retro-foreland basin since the Maastrichtian (72-66 Ma; Figs. 11 to 13). North of 5°N, no structural high or bulge limited sediment transfers and marine transgressions until the formation of the proto-retro-foreland basin (Maastrichtian; 72-66 Ma; Fig. 11). Since then, the forebulge migrated in response to lithospheric flexure (Bayonna et al., 2008). Between 1.5°N to 2°S, no forebulge formed and the retro-foreland kept a rather cylindrical structure that favored intermittent sediment exchanges between intracratonic and retro-foreland basins (Christophoul et al., 2002).

To summarize, sediment transfers between the cratonic and the proto-Andean margin basins were segmented longitudinally (i.e., in a N-S direction) by structural inheritance/tectonic reactivations. Inherited structures focused early forebulges of retro-foreland basins initiated by Andean orogenesis around the Maastrichtian. They were later abandoned as forebulges started migrating according to flexural subsidence / tectonic histories of retro-foreland basins.

5.4. Influence of mantle, lithospheric and surface processes on sediment routing systems

Following a Permian-Triassic period of far-field molasse sedimentation related mostly to the erosion of the Variscan-Appalachian orogen, the very-long wavelength (x 1000 km) asthenospheric upwelling formed an eroding superswell at the scale of northern South America and northwestern Africa. Post-Valanginian rifting of the Equatorial Atlantic imposed shorter wavelength (x 100 km) topographic controls on the sediment routing systems through

a segmented marginal upwarp system responding to the thinning of the continental lithosphere. Those topographic controls were maintained or renewed later into the Cenozoic. Comparable topographic wavelengths (x 100 km) were imposed to the sediment routing systems since the latest Cretaceous in the Andean retro-foreland domain and its junction with the cratonic domain. Those were controlled by the flexure of the cratonic lithosphere under the load of the growing Andes and modulated by sediment supplies to the retro-foreland basins. Late Miocene establishment of the modern Amazon River drainage could be a consequence of those combined processes, triggered by an increased in Andean sediment fluxes. But negative dynamic topography related to westward subducting slab dynamics under the distal retro-foreland would still have been required to achieve the modern drainage configuration (Shephard et al., 2010; Bicudo et al., 2020).

To summarize, the successive first-order configurations of the sediment routing system of northern South America were primarily set in response to very long-wavelength asthenospheric forcing and long-wavelength lithospheric-scale vertical movements that are typical of cold cratonic lithospheres.

In the Andean orogenic domain, tectonic deformation and crustal thickening were the primary drivers for erosion. By contrast, wide stable cratonic domains of low topographic gradients must have been more sensitive to climate-controlled erosion / deposition processes. Cratonic northern South America remained in the inter-tropical zone for the entire Meso-Cenozoic and was therefore subjected to chemical weathering that produced lateritic covers and duricrusts (Tardy et al., 1991), enhancing clastic sediments sequestration in soils and chemical erosional exports. Low solid exports from cratonic source areas must therefore be considered in source-to-sink budgets, particularly during greenhouse climate periods of the Early Jurassic (Holz, 2015; Figs. 5 and 6), the Late Cretaceous (i.e., the Phanerozoic peak greenhouse and global sea level; e.g., Peulvast, 2008), and the Paleogene (e.g., Prasad, 1983),

as well as the Mid-Miocene thermal optimum, whose bauxites and laterites are still preserved (Figs. 12 and 13; e.g., Vasconcelos and Carmo, 2018).

Conclusions

The mapping of the sediment sources and sinks and constraints on sediment routes allowed evaluating how the northern South American source-to-sink systems evolved under the influence of the Atlantic rifting and the active Andean margin over the last 250 My (Fig. 14). The Amazonas-Solimões trough remained a main route / transit area for sediments between the cratonic domains and the proto-Andean active margin, while other sediment pathways adapted mostly to marginal upwarps formed along the rifted Atlantic margins or the forebulges of Andean retro-foreland basins. Structurally controlled arches inherited from the Paleozoic also regulated connections between the intracratonic domain and the proto-Andean / Andean basins. A major Triassic-Early Cretaceous sedimentary hiatus indicates long-lasting asthenospheric support to an eroding superswell at the scale of northern South America and northwestern Africa. This protracted erosional regime routed sediments to the proto-Andean marginal basins, the Central Atlantic rift/rifted margins and the Saharan cratonic basin. Along the Atlantic margins of northern South America, connections of the rift and rifted margin basins with the cratonic routing system were controlled by transient rift shoulders and marginal upwarps. From the Aptian onward, the connections of the proto-Andean margin basins and later Andean retro-foreland basins with the cratonic domain were, at least partially, regulated by inherited Paleozoic structures, which were replaced by flexural forebulges of retro-foreland basins since the Maastrichtian. Enhanced lateritic weathering during greenhouse periods favored clastic sediment storage in forested soils of the cratonic domain. Accordingly, the preservation of extensive Cenozoic lateritic covers over cratonic northern South America attests to negligible solid erosional exports compared to those of the Andes

over that period. Very-long wavelength (x 1000 km) asthenospheric support, long-wavelength (x 100 km) lithospheric-scale vertical movements and climate-driven erosion processes exerted first-order controls on the northern South America cratonic sediment source-to-sink systems over geological time-scales. However, their relative contributions remain to be quantified.

Acknowledgments

This work was funded by the BRGM and TotalEnergies within the framework of the S2S project. We thank the R&D TotalEnergies group for access to subsurface data. We also thank Brian Horton for his constructive and supportive review.

References

Abinader, H.D., 2008. Depósitos cenozóicos da porção oeste da bacia do Amazonas. Master Thesis. Universidade Federal do Amazonas, Manaus, Brazil. 98pp.

Abrantes, F.R., Nogueira, A.C.R., Soares, J.L., 2016. Permian paleogeography of west-central Pangea: Reconstruction using sabkha-type gypsum-bearing deposits of Parnaíba Basin, Northern Brazil. Sedimentary Geology 341, 175-188. https://doi.org/10.1016/j.sedgeo.2016.06.004

Algar, S.T., Pindell, J.L., 1993. Structure and deformation history of the northern range of Trinidad and adjacent areas. Tectonics 12, 814-829. https://doi.org/10.1029/93TC00673

Antoine, P.-O., Roddaz, M., Brichau, S., Tejada-Lara, J., Salas-Gismondi, R., Altamirano, A., Louterbach, M., Lambs, L., Otto, T., Brusset, S., 2013. Middle Miocene vertebrates from the Amazonian Madre de Dios Subandean Zone, Perú. Journal of South American Earth Sciences 42, 91-102. https://doi.org/10.1016/j.jsames.2012.07.008

Arnaud, H., Arnaud-Vanneau, A., Bulot, L.G., Beck, C., Macsotay, O., Stephan, J.F., Vivas, V., 2000. Le Crétacé inférieur du Venezuela oriental : stratigraphie séquentielle des carbonates sur la transversale Casanay-Maturin (États de Anzoâtegui, Monagas et Sucre). Géologie Alpine 76, 3-81.

Aspden, J.A., Litherland, M., 1992. The geology and Mesozoic collisional history of the Cordillera Real, Ecuador. Tectonophysics 205, 187-204. https://doi.org/10.1016/0040-1951(92)90426-7

Assine, M.L., 2007. Bacia do Araripe. Boletim de Geociências da Petrobras 15, 371-389.

Assine, M.L., 1994. Paleocorrentes e paleogeografia na bacia do Araripe, Nordeste do Brasil. Revista Brasileira de Geociências 24, 223-232.

Atherton, M.P., Webb, S., 1989. Volcanic facies, structure, and geochemistry of the marginal basin rocks of central Peru. Journal of South American Earth Sciences 2, 241-261. https://doi.org/10.1016/0895-9811(89)90032-1

Bahia, R.B.C., Martins-Neto, M.A., Barbosa, M.S.C., Pedreira, A.J., 2006. Revisão estratigráfica bacia dos Parecis - Amazônia. Revista Brasileira de Geociências 36, 692-703.

Barragán, R., Baby, P., Duncan, R., 2005. Cretaceous alkaline intra-plate magmatism in the Ecuadorian Oriente Basin: Geochemical, geochronological and tectonic evidence. Earth and Planetary Science Letters 236, 670-690. https://doi.org/10.1016/j.epsl.2005.03.016

Bartok, P., 1993. Pre-breakup geology of the Gulf of Mexico-Caribbean: Its relation to Triassic and Jurassic rift systems of the region. Tectonics 12, 441-459. https://doi.org/10.1029/92TC01002

Bayona, G., Cortes, M., Jaramillo, C., Ojeda, G., Aristizabal, J.J., Reyes-Harker, A., 2008. An integrated analysis of an orogen-sedimentary basin pair: Latest Cretaceous-Cenozoic

evolution of the linked Eastern Cordillera orogen and the Llanos foreland basin of Colombia. Geological Society of America Bulletin 120, 1171-1197. https://doi.org/10.1130/B26187.1

Bicudo, T.C., Sacek, V., Paes de Almeida, R., 2020. Reappraisal of the relative importance of dynamic topography and Andean orogeny on Amazon landscape evolution. Earth and Planetary Science Letters 546, 116423. https://doi.org/10.1016/j.epsl.2020.116423

Balkwill, H.R., Rogrigue, G., Paredes, F.I., Almeida, J.P., 1995. Northern part of Oriente basin, Ecuador: reflection seismic expression of structures. American Association of Petroleum Geologists Memoir 62, 559-571.

Boekhout, F., Reitsma, M.J., Spikings, R., Rodriguez, R., Ulianov, A., Gerdes, A., Schaltegger, U., 2018. New age constraints on the palaeoenvironmental evolution of the late Paleozoic back-arc basin along the western Gondwana margin of southern Peru. Journal of South American Earth Sciences 82, 165-180. https://doi.org/10.1016/j.jsames.2017.12.016

Bulanova, G.P., Walter, M.J., Smith, C.B., Kohn, S.C., Armstrong, L.S., Blundy, J., Gobbo, L., 2010. Mineral inclusions in sublithospheric diamonds from Collier 4 kimberlite pipe, Juina, Brazil: subducted protoliths, carbonated melts and primary kimberlite magmatism. Contributions to Mineralogy and Petrology, 160, 489-510.

Burke, K., Steinberger, B., Torsvik, T.H., Smethurst, M.A., 2008. Plume Generation Zones at the margins of Large Low Shear Velocity Provinces on the core-mantle boundary. Earth and Planetary Science Letters 265, 49-60. https://doi.org/10.1016/j.epsl.2007.09.042

Caballero, V., Mora, A., Quintero, I., Blanco, V., Parra, M., Rojas, L.E., Lopez, C., Sánchez, N., Horton, B.K., Stockli, D., Duddy, I., 2013. Tectonic controls on sedimentation in an intermontane hinterland basin adjacent to inversion structures: the Nuevo Mundo

syncline, Middle Magdalena Valley, Colombia. Geological Society, London, Special Publication 377, 315-342. https://doi.org/10.1144/SP377.12

Campos, J.E.G., Dardenne, M.A., 1997. Estratigrafia e sedimentação da bacia Sanfranciscana: uma revisão. Revista Brasileira de Geociências 27, 269-282.

Capaldi, T.N., McKenzie, N.R., Horton, B.K., Mackaman-Lofland, C., Colleps, C.L., Stockli, D.F., 2021. Detrital zircon record of Phanerozoic magmatism in the southern Central Andes. Geosphere 17, 876–897. https://doi.org/10.1130/GES02346.1

Caixeta, J.M., Milhomen, P. da S., Witzke, R.E., Dupuy, I.S.S., Gontijo, G.A., 2007. Bacia de Camamu. Boletim de Geociências da Petrobras 15, 455-461.

Centeno-García, E., 2017. Mesozoic tectono-magmatic evolution of Mexico: An overview. Ore Geology Reviews 81, 1035-1052. https://doi.org/10.1016/j.oregeorev.2016.10.010

Chaboureau, A.-C., Guillocheau, F., Robin, C., Rohais, S., Moulin, M., Aslanian, D., 2013. Paleogeographic evolution of the central segment of the South Atlantic during Early Cretaceous times: Paleotopographic and geodynamic implications. Tectonophysics 604, 191-223. https://doi.org/10.1016/j.tecto.2012.08.025

Christophoul, F., Baby, P., Dávila, C., 2002. Stratigraphic responses to a major tectonic event in a foreland basin: the Ecuadorian Oriente Basin from Eocene to Oligocene times. Tectonophysics 345, 281-298. https://doi.org/10.1016/S0040-1951(01)00217-7

Coltice, N., Philips, B.R., Bertrand, H., Ricard, Y., Rey, P., 2007. Global warming of the mantle at the origin of flood basalts over supercontinents. Geology 35, 391-394.

Condé, V.C., Lana, C.C., da Cruz Pessoa Neto, O., Roesner, E.H., de Morais Neto, J.M., Dutra, D.C. 2007. Bacia do Ceará. Boletim de Geociências da Petrobras 15, 347-355.

Condie, K.C., 2004. Supercontinents and superplume events: distinguishing signals in the geologic record. Physics of the Earth and Planetary Interiors 146, 319-332. https://doi.org/10.1016/j.pepi.2003.04.002

Cooper, M.A., Addison, F.T., Avarez, R., Coral, M., Graham, R.H., Hayward, A.B., Howe, S., Martinez, J., Naar, J., Penas, R., Pulham, A.J., Taborda, A., 1995. Basin development and tectonic history of the Llanos basin Eastern Cordillera, and middle Magdalena Valley, Colombia. American Association of Petroleum Geologists Bulletin 79, 1421-1443.

Cordani, U.G., Ramos, V.A., Fraga, L.M., Delgado, I., de Souza, K.G., Gomes, F.E.M., Schobbenhaus, C., Cegarra, M., 2016. Tectonic map of South America (scale 1 :5,000,000). CGMW-CPRM-SEGEMAR.

Córdoba, V.C., de Sá, E.F.J., Souza, D. do C., Antunes, A.F., 2007. Bacia de Pernambuco-Paraíba. Boletim de Geociências da Petrobras 15, 391-403.

Costa, I.P., Milhomen, P.S., Vital Bueno, G., Rocha Lima e Silva, H.S., Dietzsch Kosin, M., 2007a. Sub-bacia de Tucano Sul e Central. Boletim de Geociências da Petrobras 15, 433-443.

Costa, I.P., Vital Bueno, G., Milhomen, P.S., Rocha Lima e Silva, H.S., Dietzsch Kosin, M., 2007b. Sub-bacia de Tucano Norte e Bacia de Jatobá. Boletim de Geociências da Petrobras 15, 445-453.

Craddock, J.P., Malone, D.H., Porter, R., Compton, J., Luczaj, J., Konstantinou, A., Day, J.E., Johnston, S.T., 2017. Paleozoic reactivation structures in the Appalachian-Ouachita-Marathon foreland: Far-field deformation across Pangea. Earth-Science Reviews 169, 1-34. https://doi.org/10.1016/j.earscirev.2017.04.002

Crawford, F.D., Szelewski, C.E., Alvey, G.D., 1985. Geology and exploration in the Takutu graben of Guyana and Brazil. Journal of Petroleum Geology 8, 5-36.

Custódio, M.A., Quaglio, F., Warren, L.V., Simões, M.G., Fürsich, F.T., Perinotto, J.A.J., Assine, M.L., 2017. The transgressive-regressive cycle of the Romualdo Formation (Araripe Basin): Sedimentary archive of the Early Cretaceous marine ingression in the

interior of Northeast Brazil. Sedimentary Geology 359, 1-15. https://doi.org/10.1016/j.sedgeo.2017.07.010

da Cruz da Cunha, P.R., 2007. Bacia do Acre. Boletim de Geociências da Petrobras 15, 207-215.

da Cruz da Cunha, P.R., Gonçalves de Melo, J.H., Braga da Silva, O., 2007a. Bacia do Amazonas. Boletim de Geociências da Petrobras 15, 227-251.

da Cruz Pessoa Neto, O., Soares, U.M., da Silva, J.G.F., Roesner, E.H., Florencio, C.P., de Souza, C.A.V., 2007b. Bacia Potiguar. Boletim de Geociências da Petrobras 15, 357-369.

Daemon, R.F., 1975. Contribuição à datação da formação Alter do Chão, bacía do Amazonas. Revista Brasileira de Geociências 5, 78-84.

Daemon, R.F., Contreiras, C.J.A., 1971. Zoneamento palinalógico da bacia do Amazonas. Anais do 25th Congresso Brasiliano de Geologia 3, 79-91.

Dantas, E.L., Souza, V.S., Nogueira, A.C.R., Santos, R.V., Poitrasson, F., Cruz, L.V., Mendes, A.C., 2014. U-Pb dating on detrital zircon and Nd and Hf isotopes related to the provenance of siliciclastic rocks of the Amazon Basin: Implications for the origin of Proto-Amazonas River, European Geoscience Union General Assembly, Vienna, 16328.

Dashwood, M.F., Abbotts, I.L., 1990. Aspects of the petroleum geology of the Oriente Basin, Ecuador. Geological Society, London, Special Publication 50, 89-117. https://doi.org/10.1144/GSL.SP.1990.050.01.06

de Castro, D.L., Bezerra, F.H.R., Castelo Branco, R.M.G., 2008. Geophysical evidence of crustal-heterogeneity control of fault growth in the Neocomian Iguatu basin, NE Brazil. Journal of South American Earth Sciences 26, 271-285.

Delgado, A., Mora, A., Reyes-Harker, A., 2012. Deformation partitioning in the Llanos

foreland basin during the Cenozoic and its correlation with mountain building in the hinterland. Journal of South American Earth Sciences 39, 228-244.

de Andrade Campos Neto, O.P., Souza Lima, W., Gomes Cruz, F.E., 2007. Bacia de Sergipe-Alagoas. Boletim de Geociências da Petrobras 15, 405-415.

de Matos, R.M.D., 1999. History of the northeast Brazilian rift system: kinematic implications for the break-up between Brazil and West Africa, in: The Oil and Gas Habitats of the South Atlantic. Cameron N.R., Bate R. H., Clure V. S. (Eds), Geological Society, London, Special Publication 153, 55-73.

De Min, A., Piccirillo, E.M., Marzoli, A., Bellieni, G., Renne, P.R., Ernesto, M., Marques, L.S., 2003. The Central Atlantic Magmatic Province (CAMP) in Brazil: Petrology, geochemistry, 40Ar/39Ar ages, paleomagnetism and geodynamic implications, in: Hames, W., McHone, J.G., Renne, P., Ruppel, C. (Eds.), Geophysical Monograph Series. American Geophysical Union, Washington, D. C., pp. 91-128. https://doi.org/10.1029/136GM06

Dickinson, W.R., Gehrels, G.E., Stern, R.J., 2010. Late Triassic Texas uplift preceding Jurassic opening of the Gulf of Mexico: Evidence from U-Pb ages of detrital zircons. Geosphere 6, 641-662. https://doi.org/10.1130/GES00532.1

Dickinson, W.R., Lawton, T.F., 2001. Carboniferous to Cretaceous assembly and fragmentation of Mexico. Geological Society of America Bulletin 113, 1142-1160. https://doi.org/10.1130/0016-7606(2001)113<1142:CTCAAF>2.0.CO;2

Dino, R., da Silva, O.B., Abrahao, D., 1999. Palynological and stratigraphic characterization of the Cretaceous strata from the Alter do Chao Formation, Amazonas Basin, in: Boletim Do Simposio Sobre o Cretaceo Do Brasil. 557-565.

Eakin, C.M., Lithgow-Bertelloni, C., Dávila, F.M., 2014. Influence of Peruvian flat-subduction dynamics on the evolution of western Amazonia. Earth and Planetary Science Letters 404, 250-260. https://doi.org/10.1016/j.epsl.2014.07.027

Egüez, A., Gaona, M., Albán, A., 2017. Mapa Geológico de la República del Ecuador, *Scale* 1/1,000,000, Ministerio de Minería, Instituto Nacional de Investigación Geológico Minero Met alúrgico, Quito, Ecuador.

Elías-Herrera, M., Ortega-Gutiérrez, F., 2002. Caltepec fault zone: An Early Permian dextral transpressional boundary between the Proterozoic Oaxacan and Paleozoic Acatlán complexes, southern Mexico, and regional tectonic implications. Tectonics 21, 1-18. https://doi.org/10.1029/2000TC001278

Erlich, R.N., Barrett, S.F., 1992. Petroleum geology of the Eastern Venezuela basin. American Association of Petroleum Geologists Memoir 55, 341-362.

Escalona, A., Mann, P., 2011. Tectonics, basin subsidence mechanisms, and paleogeography of the Caribbean-South American plate boundary zone. Marine and Petroleum Geology 28, 8-39. https://doi.org/10.1016/j.marpetgeo.2010.01.016

Espurt, N., Brusset, S., Baby, P., Hermoza, W., Bolaños, R., Uyen, D., Déramond, J., 2008. Paleozoic structural controls on shortening transfer in the Subandean foreland thrust system, Ene and southern Ucayali basins, Peru: shortening transfer in the Ucayali basin. Tectonics 27, TC3009. https://doi.org/10.1029/2007TC002238

Eude, A., Roddaz, M., Brichau, S., Brusset, S., Calderon, Y., Baby, P., Soula, J.-C., 2015. Controls on timing of exhumation and deformation in the northern Peruvian eastern Andean wedge as inferred from low-temperature thermochronology and balanced cross section: exhumation and deformation of North Peru. Tectonics 34, 715-730. https://doi.org/10.1002/2014TC003641

Exxon Production Research Company, 1994. Tectonic Map of the World, World Mapping Project, *Scale* 1:1,000,000, American Association of Petroleum Geologists, Tulsa, Oklahoma.

Feijó, F.J., Souza, R.G., 1994. Bacia do Acre. Boletim de Geociências da Petrobras 8, 9-16.

Figueiredo, F.T., Almeida, R.P., Freitas, B.T., Marconato, A., Carrera, S.C., Turra, B.B., 2016. Tectonic activation, source area stratigraphy and provenance changes in a rift basin: the Early Cretaceous Tucano Basin (NE-Brazil). Basin Research 28, 433-445. https://doi.org/10.1111/bre.12115

Figueiredo, J.P., Zalán, P.V., Soares, E. F., 2007. Bacia da Foz do Amazonas. Boletim de Geociências da Petrobras 15, 299-309.

Flament, N., Gurnis, M., Müller, R.D., Bower, D.J., Husson, L., 2015. Influence of subduction history on South American topography. Earth and Planetary Science Letters 430, 9-18. https://doi.org/10.1016/j.epsl.2015.08.006

Foster, T.M., Soreghan, G.S., Soreghan, M.J., Benison, K.C., Elmore, R.D., 2014. Climatic and paleogeographic significance of eolian sediment in the Middle Permian Dog Creek Shale (Midcontinent U.S.). Palaeogeography, Palaeoclimatology, Palaeoecology 402, 12-29. https://doi.org/10.1016/j.palaeo.2014.02.031

Ganne, J., Feng, X., Rey, P., De Andrade, V., 2016. Statistical petrology reveals a link between supercontinents cycle and mantle global climate. American Mineralogist 101, 2768–2773. https://doi.org/10.2138/am-2016-5868

George, S.W.M., Horton, B.K., Vallejo, C., Nogales, V., 2017. Provenance of Miocene Hinterland Basins in Ecuador: Implications for the Growth of Topographic Barriers in the Northern Andes. American Geophysical Union Fall Meeting, San Francisco, T23D-2546.

George, S.W.M., Horton, B.K., Jackson, L.J., Moreno, F., Carlotto, V., Garzione, C.N., 2019.

Sediment provenance variations during contrasting Mesozoic-early Cenozoic tectonic regimes of the northern Peruvian Andes and Santiago-Marañón foreland basin, in: Horton, B.K., Folguera, A., eds., Andean Tectonics. Elsevier, pp. 269–296. https://doi.org/10.1016/B978-0-12-816009-1.00012-5

George, S.W.M., Horton, B.K., Vallejo, C., Jackson, L.J., Gutierrez, E.G., 2021. Did accretion of the Caribbean oceanic plateau drive rapid crustal thickening in the northern Andes? Geology 49, 936–940. https://doi.org/10.1130/G48509.1

Gonçalves, F.T.T., Mora, C.A., Córdoba, F., Kairuz, E.C., Giraldo, B.N., 2002. Petroleum generation and migration in the Putumayo Basin, Colombia: insights from an organic geochemistry and basin modeling study in the foothills. Marine and Petroleum Geology 19, 711-725. https://doi.org/10.1016/S0264-8172(02)00034-X

Góes, A.M., Souza, J.M., Teixeira, L.B., 1990. The Parnaíba basin: Exploratory stage and oil perspectives. Boletim de Geociências da Petrobras 4, 55-64.

Guiraud, R., Bosworth, W., Thierry, J., Delplanque, A., 2005. Phanerozoic geological evolution of Northern and Central Africa: An overview. Journal of African Earth Sciences 43, 83-143. https://doi.org/10.1016/j.jafrearsci.2005.07.017

Gurnis, M., Mitrovica, J.X., Ritsema, J., van Heijst, H.-J., 2000. Constraining mantle density structure using geological evidence of surface uplift rates: The case of the African Superplume. Geochemistry, Geophysics. Geosystems. 1, https://doi.org/10.1029/1999GC000035

Gutiérrez, E.G., Horton, B.K., Vallejo, C., Jackson, L.J., George, S.W.M., 2019. Provenance and geochronological insights into Late Cretaceous-Cenozoic foreland basin development in the Subandean Zone and Oriente Basin of Ecuador, in: Horton, B.K., Folguera, A., eds., Andean Tectonics. Elsevier, pp. 237–268. https://doi.org/10.1016/B978-0-12-816009-1.00011-3

Gontijo, G.A., Milhomen, P.S., Caixeta, J.M., Siqueira Dupuy, I.S., de Lemos Menezes, P.E., 2007. Bacia de Almada. Boletim de Geociências da Petrobras 15, 463-473.

Graddi, J.C.S.V., Neto, O.P.A.C., Caixeta, J.M., 2007. Bacia de Jacuípe. Boletim de Geociências da Petrobras 15, 417-421.

Hamlin, H.S., 2009. Ozona sandstone, Val Verde Basin, Texas: Synorogenic stratigraphy and depositional history in a Permian foredeep basin. American Association of Petroleum Geologists Bulletin 93, 573-594. https://doi.org/10.1306/01200908121

Harman, R., Gallagher, K., Brown, R., Raza, A., Bizzi, L., 1998. Accelerated denudation and tectonic/geomorphic reactivation of the cratons of northeastern Brazil during the Late Cretaceous. Journal of Geophysical Research: Solid Earth 103, 27091-27105. https://doi.org/10.1029/98JB02524

Heine, C., Zoethout, J., Müller, R.D., 2013. Kinematics of the South Atlantic rift. Solid Earth 5, 41-116. https://doi.org/10.5194/sed-5-41-2013

Hermoza, W., Brusset, S., Baby, P., Gil, W., Roddaz, M., Guerrero, N., Bolaños, R., 2005. The Huallaga foreland basin evolution: Thrust propagation in a deltaic environment, northern Peruvian Andes. Journal of South American Earth Sciences 19, 21-34. https://doi.org/10.1016/j.jsames.2004.06.005

Holz, M., 2015. Mesozoic paleogeography and paleoclimates - A discussion of the diverse greenhouse and hothouse conditions of an alien world. Journal of South American Earth Sciences 61, 91-107. https://doi.org/10.1016/j.jsames.2015.01.001

Hoorn, C., Bogotá-A, G.R., Romero-Baez, M., Lammertsma, E.I., Flantua, S.G.A., Dantas, E.L., Dino, R., do Carmo, D.A., Chemale, F., 2017. The Amazon at sea: Onset and stages of the Amazon River from a marine record, with special reference to Neogene plant turnover in the drainage basin. Global and Planetary Change 153, 51-65. https://doi.org/10.1016/j.gloplacha.2017.02.005

Hoorn, C., Wesselingh, F.P., ter Steege, H., Bermudez, M.A., Mora, A., Sevink, J., Sanmartin, I., Sanchez-Meseguer, A., Anderson, C.L., Figueiredo, J.P., Jaramillo, C., Riff, D., Negri, F.R., Hooghiemstra, H., Lundberg, J., Stadler, T., Sarkinen, T., Antonelli, A., 2010. Amazonia Through Time: Andean Uplift, Climate Change, Landscape Evolution, and Biodiversity. Science 330, 927-931. https://doi.org/10.1126/science.1194585

Horton, B.K., 2018. Sedimentary record of Andean Mountain building. Earth-Science Reviews 178, 279-309. https://doi.org/10.1016/j.earscirev.2017.11.025

Horton, B.K., 2022. Unconformity development in retroarc foreland basins: implications for the geodynamics of Andean-type margins. Journal of the Geological Society 179, jgs2020-263. https://doi.org/10.1144/jgs2020-263

Horton, B.K., Anderson, V.J., Caballero, V., Saylor, J.E., Nie, J., Parra, M., Mora, A., 2015. Application of detrital zircon U-Pb geochronology to surface and subsurface correlations of provenance, paleodrainage, and tectonics of the Middle Magdalena Valley Basin of Colombia. Geosphere 11, 1790-1811. https://doi.org/10.1130/GES01251.1

Horton, B.K., Saylor, J.E., Nie, J., Mora, A., Parra, M., Reyes-Harker, A., Stockli, D.F., 2010. Linking sedimentation in the northern Andes to basement configuration, Mesozoic extension, and Cenozoic shortening: Evidence from detrital zircon U-Pb ages, Eastern Cordillera, Colombia. Geological Society of America Bulletin 122, 1423-1442. https://doi.org/10.1130/B30118.1

Hungerbühler, D., Steinmann, M., Winkler, W., Seward, D., Egüez, A., Peterson, D.E., Helg, U., Hammer, C., 2002. Neogene stratigraphy and Andean geodynamics of southern Ecuador. Earth-Science Reviews 57, 75-124. https://doi.org/10.1016/S0012-8252(01)00071-X

Hunt, L., Stachel, T., Morton, R., Grütter, H., Creaser, R.A., 2009. The Carolina kimberlite, Brazil — Insights into an unconventional diamond deposit. Lithos 112, 843-851. https://doi.org/10.1016/j.lithos.2009.04.018

Ismael, M., 2014. Tectonostratigraphic stages in the Mesozoic opening and subsidence of the Gulf of Mexico based on deep-penetration seismic reflection data in the salt-free eastern part of the basin. Master Thesis, University of Houston, 103p.

Iturralde-Vinent, M.A., 2006. Meso-Cenozoic Caribbean Paleogeography: Implications for the Historical Biogeography of the Region. International Geology Review 48, 791-827. https://doi.org/10.2747/0020-6814.48.9.791

Jaillard, E., 1994. Kimmeridgian to Paleocene tectonics and geodynamic evolution of the Peruvian (and Ecuadorian) margin, in: Cretaceous Tectonics of the Andes. Salfity, J.A., International Earth Evolution Sciences Monograph Series, Vieweg, Springer, Wiesbaden, 101-167. https://doi.org/10.1007/978-3-322-85472-8

Jaillard, E., 2022. Late Cretaceous-Paleogene orogenic build-up of the Ecuadorian Andes: Review and discussion. Earth-Science Reviews 230, 104033. https://doi.org/10.1016/j.earscirev.2022.104033

Jaillard, E., Lapierre, H., Ordonez, M., Alava, J.T., Amortegui, A., Vanmelle, J., 2009. Accreted oceanic terranes in Ecuador: southern edge of the Caribbean Plate? Geological Society, London Special Publication 328, 469-485. https://doi.org/10.1144/SP328.19

Jaillard, E., Soler, P., Carlier, G., Mourier, T., 1990. Geodynamic evolution of the northern and central Andes during early to middle Mesozoic times: a Tethyan model. Journal of the Geological Society 147, 1009-1022. https://doi.org/10.1144/gsjgs.147.6.1009

Jaillard, E., Bengtson, P., Dhondt, A.V., 2005. Late Cretaceous marine transgressions in Ecuador and northern Peru: A refined stratigraphic framework. Journal of South

American Earth Sciences 19, 307-323. https://doi.org/10.1016/j.jsames.2005.01.006

Jaillard, E., Ordoñez, M., Benitez, S., Berrones, G., Jiménez, N., Montenegro, G., Zambrano, I., 1995. Basin development in an accretionary, oceanic-floored fore-arc setting; Southern Coastal Ecuador during Late Cretaceous-Late Eocene time, in: Petroleum Basins of South America. Tankard, A.J., Welsink, H.J., Soruco, R.S. (Eds) American Association of Petroleum Geologists Memoir, 62, 615-631. https://doi.org/10.1306/M62593C32

Jelinek, A.R., Chemale, F., van der Beek, P.A., Guadagnin, F., Cupertino, J.A., Viana, A., 2014. Denudation history and landscape evolution of the northern East-Brazilian continental margin from apatite fission-track thermochronology. Journal of South American Earth Sciences 54, 158-181. https://doi.org/10.1016/j.jsames.2014.06.001

Labails, C., Olivet, J.-L., Aslanian, D., Roest, W.R., 2010. An alternative early opening scenario for the Central Atlantic Ocean. Earth and Planetary Science Letters 297, 355-368. https://doi.org/10.1016/j.epsl.2010.06.024

Laya, J.C., Tucker, M.E., 2012. Facies analysis and depositional environments of Permian carbonates of the Venezuelan Andes: Palaeogeographic implications for Northern Gondwana. Palaeogeography, Palaeoclimatology, Palaeoecology 331-332, 1-26. https://doi.org/10.1016/j.palaeo.2012.02.011

Linol, B., de Wit, M.J., Barton, E., de Wit, M.J.C., Guillocheau, F., 2016. U-Pb detrital zircon dates and source provenance analysis of Phanerozoic sequences of the Congo Basin, central Gondwana. Gondwana Research 29, 208-219. https://doi.org/10.1016/j.gr.2014.11.009

Linol, B., de Wit, M.J., Barton, E., Guillocheau, F., de Wit, M.C.J., Colin, J.-P., 2015a. Facies analyses, chronostratigraphy and paleo-environmental reconstructions of Jurassic to Cretaceous sequences of the Congo Basin, in: de Wit, M.J., Guillocheau, F., (Eds.)

Geology and Resource Potential of the Congo Basin. Springer, Berlin, pp. 135-161. https://doi.org/10.1007/978-3-642-29482-2_8

Linol, B., de Wit, M.J., Barton, E., Guillocheau, F., de Wit, M.C.J., Colin, J.-P., 2015b. Paleogeography and tectono-stratigraphy of Carboniferous-Permian and Triassic 'Karoo-Like' Sequences of the Congo Basin, in: de Wit, M.J., Guillocheau, F., (Eds) Geology and Resource Potential of the Congo Basin. Springer, Berlin, pp. 111-134. https://doi.org/10.1007/978-3-642-29482-2_7

Linol, B., de Wit, M.J., Milani, E.J., Guillocheau, F., Scherer, C., 2015c New Regional Correlations Between the Congo, Paraná and Cape-Karoo Basins of Southwest Gondwana, in: de Wit, M.J., Guillocheau, F., (Eds.) Geology and Resource Potential of the Congo Basin. Springer, Berlin, pp. 245-268. https://doi.org/10.1007/978-3-642-29482-2_13

Loparev, A., Rouby, D., Chardon, D., Dall'Asta, M., Sapin, F., Bajolet, F., Ye, J., Paquet, F., 2021. Superimposed Rifting at the Junction of the Central and Equatorial Atlantic: Formation of the Passive Margin of the Guiana Shield. Tectonics 40, e2020TC006159. https://doi.org/10.1029/2020TC006159

Louterbach, M., Roddaz, M., Antoine, P.-O., Marivaux, L., Adnet, S., Bailleul, J., Dantas, E., Santos, R.V., Chemale, F., Baby, P., Sanchez, C., Calderon, Y., 2018. Provenance record of Late Maastrichtian-Late Palaeocene Andean Mountain building in the Amazonian retroarc foreland basin (Madre de Dios basin, Peru). Terra Nova 30, 17-23. https://doi.org/10.1111/ter.12303

Louterbach, M., Roddaz, M., Bailleul, J., Antoine, P.-O., Adnet, S., Kim, J.H., van Soelen, E., Parra, F., Gérard, J., Calderon, Y., Gagnaison, C., Sinninghe Damsté, J.S., Baby, P., 2014. Evidences for a Paleocene marine incursion in southern Amazonia (Madre de Dios Sub-Andean Zone, Peru). Palaeogeography, Palaeoclimatology, Palaeoecology

414, 451-471. https://doi.org/10.1016/j.palaeo.2014.09.027

Macellari, C.E., 1988. Cretaceous paleogeography and depositional cycles of western South America. Journal of South American Earth Sciences 1, 373-418. https://doi.org/10.1016/0895-9811(88)90024-7

MacRae, G., Watkins, J.S., 1995. Early Mesozoic rift stage half graben formation beneath the DeSoto Canyon salt basin, northeastern Gulf of Mexico. Journal of Geophysical Research 100, 17795-17812.

Mann, P., Escalona, A., Verónica, M., 2006. Regional geologic and tectonic setting of the Maracaibo supergiant basin, western Venezuela. American Association of Petroleum Geologists Bulletin 90, 445-477. https://doi.org/10.1306/10110505031

Mapes, R.W., 2009. Past and present provenance of the Amazon River. PhD Thesis. University of North Carolina, Chapel Hill, 195p.

Mapes, R.W., Coleman, D.S., Nogueira, A.C.R., Leguizamon Vega, A.M., Abinader, H.D., 2007. Continent wide drainage inversion and significance of the Purus Arch: detrital zircon geochronology of Cretaceous and Tertiary surficial deposits of the Amazon basin, Anais XI Congresso Da ABEQUA, Belém, Brazil.

Martínez, W.V., Morales, M.R., Díaz, G.H., Milla, D.S., Montoya, C.P., Huayhua, J.R., Romero, L.P., Raymundo, T.S., 1999. Geología de los cuadrángulos de Bolívar, Curaray, Santa Clotilde, Quebrada Aguablanca, Qubrada Sabaloyacu, San Lorenzo, Intuto, Río Pintoyacu, Río Mazan, Río Corrientes, Libertad, Río Nanay, Santa Rosa, Yacumama, Río Itaya, Yanayacu, Chapajilla y Nauta. Boletin del Instituto Geológico Minero y Metalúrgico, Serie A: Carta Geológica Nacional 131, 341p.

Martin-Gombojav, N., Winkler, W., 2008. Recycling of Proterozoic crust in the Andean Amazon foreland of Ecuador: implications for orogenic development of the Northern Andes: Multiple recycling of Proterozoic crust in the Northern Andes. Terra Nova 20,

22-31. https://doi.org/10.1111/j.1365-3121.2007.00782.x

Martinod, J., Gérault, M., Husson, L., and Regard, V., 2020, Widening of the Andes: An interplay between subduction dynamics and crustal wedge tectonics. Earth-Science Reviews, 204, 103170. doi:10.1016/j.earscirev.2020.103170.

Marzoli, A., 1999. Extensive 200-million-year-old continental flood basalts of the Central Atlantic Magmatic Province. Science 284, 616-618. https://doi.org/10.1126/science.284.5414.616

Masun, K.M., Smith, B.H.S., 2008. The Pimenta Bueno kimberlite field, Rondônia, Brazil: Tuffisitic kimberlite and transitional textures. Journal of Volcanology and Geothermal Research 174, 81-89. https://doi.org/10.1016/j.jvolgeores.2007.12.043

Mathalone, J., Montoya, M., 1995. Petroleum geology of the sub-andean basins of Peru. American Association of Petroleum Geologists Memoir 62, 423-441.

Matthews, K.J., Maloney, K.T., Zahirovic, S., Williams, S.E., Seton, M., Müller, R.D., 2016. Global plate boundary evolution and kinematics since the late Paleozoic. Global and Planetary Change 146, 226-250. https://doi.org/10.1016/j.gloplacha.2016.10.002

Matsuda, N.S., Dino, R., Wanderley-Filho, J.R., 2004. Revisão litoestratigráfica do Grupo Tapajós, Carbonífero Médio - Permiano da Bacia do Amazonas. Boletim de Geociências da Petrobras 12, 435-441.

May, P.R., 1971. Pattern of Triassic-Jurassic diabase dikes around the North Atlantic in the context of predrift position of the continents. Geological Society of America Bulletin 82, 1285-1292.

Mendes, A., Salomão, G., Nogueira, A., Dantas, E.L., 2015. Provenance of the Alter do Chão formation in Amazonas state (Itacoatiara-Parintins cities), Amazonas basin, Brazil, XV Congresso Brasileiro de Geoquímica, Brasilia, Brazil.

Mendes, A.C., 2013. Paleoenvironmental reconstruction of Cretaceous rocks of the Amazonas

Basin: preliminary researches, Clim-Amazon 2nd Workshop, Brasilia, Brazil.

Mendes, A.C., Truckenbrod, W., Nogueira, A.C.R., 2012. Análise faciológica da Formação Alter do Chão (Cretáceo, Bacia do Amazonas), próximo à cidade de Óbidos, Pará, Brasil. Revista Brasileira de Geociências 42, 39-57.

Merle, R., Marzoli, A., Bertrand, H., Reisberg, L., Verati, C., Zimmermann, C., Chiaradia, M., Bellieni, G., Ernesto, M., 2011. 40Ar/39Ar ages and Sr-Nd-Pb-Os geochemistry of CAMP tholeiites from Western Maranhão basin (NE Brazil). Lithos 122, 137-151. https://doi.org/10.1016/j.lithos.2010.12.010

Milani, E.J., Gonçalves de Melo, J.H., de Souza, P.A., Fernandes, L.A., França, A.B., 2007. Bacia do Paraná. Boletim de Geociências da Petrobras 15, 265-287.

Mišković, A., Spikings, R.A., Chew, D.M., Košler, J., Ulianov, A., Schaltegger, U., 2009. Tectonomagmatic evolution of Western Amazonia: Geochemical characterization and zircon U-Pb geochronologic constraints from the Peruvian Eastern Cordilleran granitoids. Geological Society of America Bulletin 121, 1298-1324. https://doi.org/10.1130/B26488.1

Mizusaki, A.M.P., Thomaz-Filho, A., Milani, E.J., de Césero, P., 2002. Mesozoic and Cenozoic igneous activity and its tectonic control in northeastern Brazil. Journal of South American Earth Sciences 15, 183-198. https://doi.org/10.1016/S0895-9811(02)00014-7

Montes, C., Rodriguez-Corcho, A.F., Bayona, G., Hoyos, N., Zapata, S., Cardona, A., 2019. Continental margin response to multiple arc-continent collisions: The northern Andes-Caribbean margin. Earth-Science Reviews 198, 102903. https://doi.org/10.1016/j.earscirev.2019.102903

Moreno, F., Garzione, C.N., George, S.W.M., Horton, B.K., Williams, L., Jackson, L.J., Carlotto, V., Richter, F., Bandeian, A., 2020. Coupled Andean Growth and Foreland

Basin Evolution, Campanian–Cenozoic Bagua Basin, Northern Peru. Tectonics 39, e2019TC005967. https://doi.org/10.1029/2019TC005967

Moreno-López, M.C., Escalona, A., 2015. Precambrian-Pleistocene tectono-stratigraphic evolution of the southern Llanos basin, Colombia. American Association of Petroleum Geologists Bulletin 99, 1473-1501. https://doi.org/10.1306/11111413138

Morgan, W.J., 1983. Hotspot tracks and the early rifting of the Atlantic. Tectonophysics 94, 123-139.

Mosmann, R., Falkenhein, F.U.H., Gonçalves, A., Nepomuceno Filho, F., 1986. Oil and gaz potential of the Amazon Paleozoic basins, in: Future Petroleum Provinces of the World. Halbouty, M.T. (Ed.) American Association of Petroleum Geologists Memoir 40, 207-241.

Moulin, M., Aslanian, D., Unternehr, P., 2010. A new starting point for the South and Equatorial Atlantic Ocean. Earth-Science Reviews 98, 1-37. https://doi.org/10.1016/j.earscirev.2009.08.001

Nascimento, M. dos S., Góes, A.M., Macambira, M.J.B., Brod, J.A., 2007. Provenance of Albian sandstones in the São Luís-Grajaú Basin (northern Brazil) from evidence of Pb-Pb zircon ages, mineral chemistry of tourmaline and palaeocurrent data. Sedimentary Geology 201, 21-42. https://doi.org/10.1016/j.sedgeo.2007.04.005

Nie, J., Horton, B.K., Saylor, J.E., Mora, A., Mange, M., Garzione, C.N., Basu, A., Moreno, C.J., Caballero, V., Parra, M., 2012. Integrated provenance analysis of a convergent retroarc foreland system: U-Pb ages, heavy minerals, Nd isotopes, and sandstone compositions of the Middle Magdalena Valley basin, northern Andes, Colombia. Earth-Science Reviews 110, 111-126. https://doi.org/10.1016/j.earscirev.2011.11.002

Nuns, J.A., Aires, J.R., 1984. Subsidence history and tectonic evolution of the Middle Amazon basin, Brazil, Petrobras-Internal Report.

Parra, M., Mora, A., Jaramillo, C., Strecker, M.R., Sobel, E.R., Quiroz, L., Rueda, M., Torres, V., 2009. Orogenic wedge advance in the northern Andes: Evidence from the Oligocene-Miocene sedimentary record of the Medina Basin, Eastern Cordillera, Colombia. Geological Society of America Bulletin 121, 780-800. https://doi.org/10.1130/B26257.1

Parnaud, F., Gou, Y., Pascual, J.-C., Capello, M.A., Truskowski, I., Passalacqua, H., 1995. Stratigraphic synthesis of Westen Venezuela, in: Petroleum Basins of South America. Tankard, A.J., Welsink, H.J., Soruco, R.S. (Eds.) American Association of Petroleum Geologists Memoir 62, 681-698.

Peace, A.L., Phethean, J.J.J., Franke, D., Foulger, G.R., Schiffer, C., Welford, J.K., McHone, G., Rocchi, S., Schnabel, M., Doré, A.G., 2020. A review of Pangaea dispersal and Large Igneous Provinces - In search of a causative mechanism. Earth-Science Reviews 206, 102902. https://doi.org/10.1016/j.earscirev.2019.102902

Pfiffner, O.A., Gonzalez, L., 2013. Mesozoic-Cenozoic Evolution of the Western Margin of South America: Case Study of the Peruvian Andes. Geosciences 3, 262-310. https://doi.org/10.3390/geosciences3020262

Pindell, J.L., 1985. Alleghenian reconstruction and subsequent evolution of the Gulf of Mexico, Bahamas, and Proto-Caribbean. Tectonics 4, 1-39. https://doi.org/10.1029/TC004i001p00001

Pindell, J.L., Kennan, L., 2009. Tectonic evolution of the Gulf of Mexico, Caribbean and northern South America in the mantle reference frame: an update. Geological Society, London, Special Publication 328, 1-55. https://doi.org/10.1144/SP328.1

Pindell, J.L., Tabbutt, K.D., 1995. Mesozoic-Cenozoic Andean paleogeography and regional controls on hydrocarbon systems. American Association of Petroleum Geologists Memoir 62, 101-128.

Peulvast, J.P., Claudino Sales, V., Bétard, F., Gunnell, Y., 2008. Low post-Cenomanian denudation depths across the Brazilian Northeast. Global and Planetary Change 62, 39-60.

Prasad, G., 1983. A review of the early Tertiary bauxite event in South America, Africa nad India. Journal of African Earth Sciences 1, 305-313.

Rangel, H.D., Flores de Oliveira, J.L., Caixeta, J.M., 2007. Bacia de Jequitinhonha. Boletim de Geociências da Petrobras 15, 475-483.

Reis, H.L.S., Alkmim, F.F., Fonseca, R.C.S., Nascimento, T.C., Suss, J.F., Prevatti, L.D., 2017. The São Francisco Basin, in: São Francisco Craton, Eastern Brazil: Tectonic Genealogy of a Miniature Continent. Heilbron, M., Cordani, U.G., Alkmim, F.F. (Eds.) Springer International Publishing, Switzerland, pp. 117-143. https://doi.org/10.1007/978-3-319-01715-0_7

Reyes-Harker, A., Ruiz-Valdivieso, C.F., Mora, A., Ramírez-Arias, J.C., Rodriguez, G., de la Parra, F., Caballero, V., Parra, M., Moreno, N., Horton, B.K., Saylor, J.E., Silva, A., Valencia, V., Stockli, D., Blanco, V., 2015. Hyperspectral imaging for the determination of bitumen content in Athabasca oil sands core samples. American Association of Petroleum Geologists Bulletin 99, 1407-1453. https://doi.org/10.1306/06181411110

Roddaz, M., Christophoul, F., Burgos Zambrano, J.D., Soula, J.-C., Baby, P., 2012. Provenance of Late Oligocene to Quaternary sediments of the Ecuadorian Amazonian foreland basin as inferred from major and trace element geochemistry and Nd-Sr isotopic composition. Journal of South American Earth Sciences 37, 136-153. https://doi.org/10.1016/j.jsames.2012.02.008

Roddaz, M., Viers, J., Brusset, S., Baby, P., Hérail, G., 2005. Sediment provenances and drainage evolution of the Neogene Amazonian foreland basin. Earth and Planetary

Science Letters 239, 57-78. https://doi.org/10.1016/j.epsl.2005.08.007

Roddaz, M., Hermoza, W., Mora, A., Baby, P., Parra, M., Christophoul, F., Brusset, S., Espurt, N., 2010. Cenozoic sedimentary evolution of the Amazonian foreland basin system, in: Amazonia: Landscape and Species Evolution: A Look into the Past. Hoorn, C., Wesselingh, F.P. (Eds.) Blackwell Publishing, Hoboken, NJ, pp. 61-88.

Roddaz, M., Viers, J., Brusset, S., Baby, P., Boucayrand, C., Hérail, G., 2006. Controls on weathering and provenance in the Amazonian foreland basin: Insights from major and trace element geochemistry of Neogene Amazonian sediments. Chemical Geology 226, 31-65. https://doi.org/10.1016/j.chemgeo.2005.08.010

Romanowicz, B., Gung, Y., 2002. Superplumes from the core-mantle boundary of the lithosphere: implications for heat flux. Science 296, 513-516.

Rosas, S., Fontboté, L., Tankard, A., 2007. Tectonic evolution and paleogeography of the Mesozoic Pucará Basin, central Peru. Journal of South American Earth Sciences 24, 1-24. https://doi.org/10.1016/j.jsames.2007.03.002

Rossetti, D.F., Bezerra, F.H.R., Dominguez, J.M.L., 2013. Late Oligocene-Miocene transgressions along the Equatorial and Eastern margins of Brazil. Earth-Science Reviews 123, 87-112. https://doi.org/10.1016/j.earscirev.2013.04.005

Rossetti, D.F., Netto, R.G., 2006. First evidence of marine influence in the Cretaceous of the Amazonas Basin, Brazil. Cretaceous Research 27, 513-528. https://doi.org/10.1016/j.cretres.2005.10.014

Rossetti, D.F., 2001. Late Cenozoic sedimentary evolution in northeastern Para, Brazil, within the context of sea level changes. Journal of South American Earth Sciences 14, 77-89.

Rubert, R.R., Mizusaki, A.M.P., Martinelli, A.G., Urban, C., 2017. Paleoenvironmental reconstruction and evolution of an Upper Cretaceous lacustrine-fluvial-deltaic sequence in the Parecis Basin, Brazil. Journal of South American Earth Sciences 80,

512-528. https://doi.org/10.1016/j.jsames.2017.10.013

Ruiz, G.M.H., Seward, D., Winkler, W., 2004. Detrital thermochronology - a new perspective on hinterland tectonics, an example from the Andean Amazon Basin, Ecuador. Basin Research 16, 413-430. https://doi.org/10.1111/j.1365-2117.2004.00239.x

Ruiz-Martínez, V.C., Torsvik, T.H., van Hinsbergen, D.J.J., Gaina, C., 2012. Earth at 200Ma: Global palaeogeography refined from CAMP palaeomagnetic data. Earth and Planetary Science Letters 331-332, 67-79. https://doi.org/10.1016/j.epsl.2012.03.008

Sacek, V., 2014. Drainage reversal of the Amazon River due to the coupling of surface and lithospheric processes. Earth and Planetary Science Letters 401, 301-312. https://doi.org/10.1016/j.epsl.2014.06.022

Sánchez, A.F., Chira, J.F., Romero, D.F., De la Cruz, J.W., Herrera, I.T., Cervante, J.G., Monge, R.M., Valencia, M.M., Cuba, A.M., 1999. Geología de los cuadrángulos de Puerto Arturo, Flor de Agosto, San Antonio des Estrecho, Nuevo Perú, San Felipe, Río Algodón, Quebrada Airambo, Mazán, Francisco de Orellana, Huanta, Iquitos, Río Maniti, Yanashi, Tamshiyacu, Río Tamshiyacu, Buenjardin, Ramon Castilla, Río Yavarí Mirin y Buenavista. Boletin del Instituto Geológico Minero y Metalúrgico, Serie A: Carta Geológica Nacional 132, 320p.

Sapin, F., Davaux, M., Dall'asta, M., Lahmi, M., Baudot, G., Ringenbach, J.-C., 2016. Post-rift subsidence of the French Guiana hyper-oblique margin: from rift-inherited subsidence to Amazon deposition effect, Geological Society, London, Special Publication 431, 125-144. https://doi.org/10.1144/SP431.11

Sarmiento-Rojas, L.F., Van Wess, J.D., Cloetingh, S., 2006. Mesozoic transtensional basin history of the Eastern Cordillera, Colombian Andes: Inferences from tectonic models. Journal of South American Earth Sciences 21, 383-411. https://doi.org/10.1016/j.jsames.2006.07.003

Saylor, J.E., Horton, B.K., Nie, J., Corredor, J., Mora, A., 2011. Evaluating foreland basin partitioning in the northern Andes using Cenozoic fill of the Floresta basin, Eastern Cordillera, Colombia: Cenozoic partitioning of the Floresta basin, Colombia. Basin Research 23, 377-402. https://doi.org/10.1111/j.1365-2117.2010.00493.x

Scherer, C.M.S., Jardim de Sá, E.F., Córdoba Centurion, V., Sousa do Carmo, D., Aquino Martins, M., Canelas Cardoso, F.M., 2014. Tectono-stratigraphic evolution of the Upper Jurassic–Neocomian rift succession, Araripe Basin, Northeast Brazil. Journal of South American Earth Sciences 49, 106-122.

Scherer, C.M.S., Goldberg, K., Bardola, T., 2015. Facies architecture and sequence stratigraphy of an early post-rift fluvial succession, Aptian Barbalha Formation, Araripe Basin, northeastern Brazil. Sedimentary Geology 322, 43-62. https://doi.org/10.1016/j.sedgeo.2015.03.010

Scherrenberg, A.F., Holcombe, R.J., Rosenbaum, G., 2014. The persistence and role of basin structures on the 3D architecture of the Marañón Fold-Thrust Belt, Peru. Journal of South American Earth Sciences 51, 45-58. https://doi.org/10.1016/j.jsames.2013.12.007

Scherrenberg, A.F., Jacay, J., Holcombe, R.J., Rosenbaum, G., 2012. Stratigraphic variations across the Marañón Fold-Thrust Belt, Peru: Implications for the basin architecture of the West Peruvian Trough. Journal of South American Earth Sciences 38, 147-158. https://doi.org/10.1016/j.jsames.2012.06.006

Schütte, P., Chiaradia, M., Beate, B., 2010. Geodynamic controls on Tertiary arc magmatism in Ecuador: Constraints from U-Pb zircon geochronology of Oligocene-Miocene intrusions and regional age distribution trends. Tectonophysics 489, 159-176. https://doi.org/10.1016/j.tecto.2010.04.015

Schwartz, J.J., Gromet, L.P., Miró, R., 2008. Timing and Duration of the Calc- Alkaline Arc

of the Pampean Orogeny: Implications for the Late Neoproterozoic to Cambrian Evolution of Western Gondwana. The Journal of Geology 116, 39–61. https://doi.org/10.1086/524122

Sempere, T., 1995. Phanerozoic evolution of Bolivia and adjacent regions, American Association of Petroleum Geologists Memoir 62, 207-230. https://doi.org/10.1306/M62593C9

Sempere, T., Carlier, G., Soler, P., Fornari, M., Carlotto, V., Jacay, J., Jiménez, N., 2002. Late Permian–Middle Jurassic lithospheric thinning in Peru and Bolivia, and its bearing on Andean-age tectonics. Tectonophysics 345, 153–181.

Seton, M., Müller, R.D., Zahirovic, S., Gaina, C., Torsvik, T., Shephard, G., Talsma, A., Gurnis, M., Turner, M., Maus, S., Chandler, M., 2012. Global continental and ocean basin reconstructions since 200 Ma. Earth-Science Reviews 113, 212-270. https://doi.org/10.1016/j.earscirev.2012.03.002

Sgarbi, G.N.C., 2000. The Cretaceous Sanfranciscan basin, eastern plateau of Brazil. Revista Brasileira de Geociências 30, 450-452.

Shephard, G.E., Müller, R.D., Liu, L., Gurnis, M., 2010. Miocene drainage reversal of the Amazon River driven by plate-mantle interaction. Nature Geoscience 3, 870-875. https://doi.org/10.1038/ngeo1017

Silva, A., Mora, A., Caballero, V., Rodriguez, G., Ruiz, C., Moreno, N., Parra, M., Ramirez-Arias, J.C., Ibáñez, M., Quintero, I., 2013. Basin compartmentalization and drainage evolution during rift inversion: evidence from the Eastern Cordillera of Colombia. Geological Society, London, Special Publication 377, 369-409. https://doi.org/10.1144/SP377.15

Silva, O.B., Caixeta, J.M., Milhomen, P.S., Dietzsch Kosin, M., 2007. Bacia do Recôncavo. Boletim de Geociências da Petrobras 15, 423-431.

Silveira, F.V., 2006. Magmatismo cenozóico da porção central do Rio Grande do Norte, NE do Brasil. PhD Thesis, Universidade Federal do Rio Grande do Norte, Natal, 220p.

Simões, M.G., Matos, S.A., Warren, L.V., Assine, M.L., Riccomini, C., Bondioli, J.G., 2016. Untold muddy tales: Paleoenvironmental dynamics of a "barren" mudrock succession from a shallow Permian epeiric sea. Journal of South American Earth Sciences 71, 223-234. https://doi.org/10.1016/j.jsames.2016.08.002

Soares, E.F., Zalán, P.V., Picanço de Figueiredo, J. de J., Trosdtorf Junior, I., 2007. Bacia do Pará-Maranhão. Boletim de Geociências da Petrobras 15, 321-329.

Soler, P., Bonhomme, M.G., 1990. Relation of magmatic activity to plate dynamics in central Peru from Late Cretaceous to present. Geological Society of America Special Paper 241, 173-192.

Soreghan, G.S., Soreghan, M.J., 2013. Tracing clastic delivery to the Permian Delaware Basin, U.S.A.: Implications for paleogeography and circulation in westernmost Equatorial Pangea. Journal of Sedimentary Research 83, 786-802. https://doi.org/10.2110/jsr.2013.63

Spikings, R., Cochrane, R., Villagomez, D., Van der Lelij, R., Vallejo, C., Winkler, W., Beate, B., 2015. The geological history of northwestern South America: from Pangaea to the early collision of the Caribbean Large Igneous Province (290-75Ma). Gondwana Research 27, 95-139. https://doi.org/10.1016/j.gr.2014.06.004

Spikings, R., Reitsma, M.J., Boekhout, F., Mišković, A., Ulianov, A., Chiaradia, M., Gerdes, A., Schaltegger, U., 2016. Characterisation of Triassic rifting in Peru and implications for the early disassembly of western Pangaea. Gondwana Research 35, 124-143. https://doi.org/10.1016/j.gr.2016.02.008

Sweet, A.C., Soreghan, G.S., Sweet, D.E., Soreghan, M.J., Madden, A.S., 2013. Permian dust in Oklahoma: Source and origin for Middle Permian (Flowerpot-Blaine) redbeds in

Western Tropical Pangaea. Sedimentary Geology 284-285, 181-196. https://doi.org/10.1016/j.sedgeo.2012.12.006

Szatmari, P., 1983. Amazon rift and Pisco-Jurua fault: Their relation to the separation of North America from Gondwana. Geology, 11, 300-304.

Talawani, M., 2002. The Orinoco heavy oil belt in Venezuela (or heavy oil to the rescue?). PhD These, Rice University, Houston.

Tappe, S., Smart, K., Torsvik, T., Massuyeau, M., de Wit, M., 2018. Geodynamics of kimberlites on a cooling Earth: Clues to plate tectonic evolution and deep volatile cycles. Earth and Planetary Science Letters 484, 1-14. https://doi.org/10.1016/j.epsl.2017.12.013

Tardy, Y., Kobilsek, B., Paquet, H., 1991. Mineralogical composition and geographical distribution of African and Brazilian periatlantic laterites. The influence of continental drift and tropical paleoclimates during the past 150 Myr and implications for India and Australia. Journal of African Earth Sciences 12, 283-295.

Tardy, Y., Roquin, C., 1998. Les latérites du Brésil et d'Amérique du Sud, in: Dérive Des Continents, Paléoclimats et Alterations Tropicales. Editions B.R.G.M. Orléans, France.

Torres, R., Ruiz, J., Patchett, J.P., Grajales, M.J., 1999. Permo-Triassic continental arc in eastern Mexico: tectonic implications for reconstructions of southern North America. Geological Society of America Special Paper 340, 191-196.

Torsvik, T.H., Cocks, L.R.M., 2013. Gondwana from top to base in space and time. Gondwana Research 24, 999-1030. https://doi.org/10.1016/j.gr.2013.06.012

Trosdtorf I. (Junior), Zalán, P.V., Figueiredo, J.J.P., Soares, E.F., 2007. Bacia de Barreirinhas. Boletim de Geociências da Petrobras 15, 331-339.

Valença, L.M.M., Neumann, V.H., Mabesoone, J.M., 2003. An overview on Callovian-

Cenomanian intracratonic basins of Northeast Brazil: Onshore stratrigraphic record of the opening of the southern Atlantic. Geologica Acta 1, 261-275.

Vallejo, C., Tapia, D., Gaibor, J., Steel, R., Cardenas, M., Winkler, W., Valdez, A., Esteban, J., Figuera, M., Leal, J., Cuenca, D., 2017. Geology of the Campanian M1 sandstone oil reservoir of eastern Ecuador: A delta system sourced from the Amazon Craton. Marine and Petroleum Geology 86, 1207-1223. https://doi.org/10.1016/j.marpetgeo.2017.07.022

Vallejo, C., Spikings, R.A., Horton, B.K., Luzieux, L., Romero, C., Winkler, W., Thomsen, T.B., 2019. Late Cretaceous to Miocene stratigraphy and provenance of the coastal forearc and Western Cordillera of Ecuador: Evidence for accretion of a single oceanic plateau fragment, in: Horton, B.K., Folguera, A., eds., Andean Tectonics. Elsevier, pp. 209–236. https://doi.org/10.1016/B978-0-12-816009-1.00010-1

van der Lelij, R., Spikings, R., Ulianov, A., Chiaradia, M., Mora, A., 2016a. Palaeozoic to Early Jurassic history of the northwestern corner of Gondwana, and implications for the evolution of the Iapetus, Rheic and Pacific Oceans. Gondwana Research 31, 271-294. https://doi.org/10.1016/j.gr.2015.01.011

van der Lelij, R., Spikings, R., Mora, A., 2016b. Thermochronology and tectonics of the Mérida Andes and the Santander Massif, NW South America. Lithos 248-251, 220-239. https://doi.org/10.1016/j.lithos.2016.01.006

Varejão, F.G., Warren, L.V., Perinotto, J.A. de J., Neumann, V.H., Freitas, B.T., Almeida, R.P. de, Assine, M.L., 2016. Upper Aptian mixed carbonate-siliciclastic sequences from Tucano Basin, Northeastern Brazil: Implications for paleogeographic reconstructions following Gondwana break-up. Cretaceous Research 67, 44-58. https://doi.org/10.1016/j.cretres.2016.06.014

Vasconcelos, P.M., Carmo, I. de O., 2018. Calibrating denudation chronology through

$^{40}Ar/^{39}Ar$ weathering geochronology. Earth-Science Reviews 179, 411-435. https://doi.org/10.1016/j.earscirev.2018.01.003

Vásquez, M., Altenberger, U., 2005. Mid-Cretaceous extension-related magmatism in the eastern Colombian Andes. Journal of South American Earth Sciences 20, 193-210. https://doi.org/10.1016/j.jsames.2005.05.010

Vaz, P.T., Rezende, N.G.A.M., Filho, J.R.W., Travassos, W.A.S., 2007a. Bacia do Parnaíba. Boletim de Geociências da Petrobras 15, 253-263.

Vaz, Pekim Tenório, Wanderley-Filho, J.R., Bueno, G.V., 2007b. Bacia do Tacutu. Boletim de Geociências da Petrobras 15, 289-297.

Villamil, T., 1999. Campanian-Miocene tectonostratigraphy, depocenter evolution and basin development of Colombia and western Venezuela. Palaeogeography, Palaeoclimatology, Palaeoecology 153, 239-275. https://doi.org/10.1016/S0031-0182(99)00075-9

Wanderley-Filho, J.R., Eiras, J.F., Vaz, P.T., 2007. Bacia do Solimões. Boletim de Geociências da Petrobras 15, 217-225.

Wanderley-Filho, J.R., Travassos, W.A.S., Alves, D.B., 2005. O diabásio nas bacias paleozóicas amazônicas - herói ou vilão? Boletim de Geociências da Petrobras 14, 177-184.

Wanderley-Filho, J.R., Eiras, J.F., Cunha, P.R.C., van der Ven, P.H., 2010. The Paleozoic Solimões and Amazonas basins and the Acre foreland basin of Brazil, in: Amazonia: Landscape and Species Evolution: A Look into the Past. Hoorn, C., Wesselingh, F.P. (Eds.) Blackwell Publishing, Hoboken, NJ, 29-37.

Watts, A.B., Rodger, M., Peirce, C., Greenroyd, C.J., Hobbs, R.W., 2009. Seismic structure, gravity anomalies, and flexure of the Amazon continental margin, NE Brazil. Journal of Geophysical Research 114, B07103. https://doi.org/10.1029/2008JB006259

Weber, B., Iriondo, A., Premo, W.R., Hecht, L., Schaaf, P., 2007. New insights into the history and origin of the southern Maya block, SE México: U-Pb-SHRIMP zircon geochronology from metamorphic rocks of the Chiapas massif. International Journal of Earth Sciences 96, 253-269. https://doi.org/10.1007/s00531-006-0093-7

White, H.J., Skopec, R.A., Ramirez, F.A., Rodas, J.A., Bonilla, G., 1995. Reservoir Characterization of the Hollin and Napo Formations, Western Oriente Basin, Ecuador. American Association of Petroleum Geologists Memoir 62, 573-596.

Winter, L.S., Tosdal, R.M., Mortensen, J.K., Franklin, J.M., 2010. Volcanic Stratigraphy and Geochronology of the Cretaceous Lancones Basin, Northwestern Peru: Position and Timing of Giant VMS Deposits. Economic Geology 105, 713-742. https://doi.org/10.2113/gsecongeo.105.4.713

Ye, J., Chardon, D., Rouby, D., Guillocheau, F., Dall'Asta, M., Ferry, J.-N., Broucke, O., 2017. Paleogeographic and structural evolution of northwestern Africa and its Atlantic margins since the early Mesozoic. Geosphere 13, 1254-1284. https://doi.org/10.1130/GES01426.1

Zalán, P.V., Matsuda, N.S., 2007. Bacia do Marajó. Boletim de Geociências da Petrobras 15, 311-319.

Zalán, P.V., Silva, P.C.R., 2007. Bacia do São Francisco. Boletim de Geociências da Petrobras 15, 561-571.

Zalán, P.V., 2007. Bacias de Bragança-Viseu, São Luís e Ilha Nova. Boletim de Geociências da Petrobras 15, 341-345.

Tables captions

Table 1. References to the published works used for the geological reconstructions (Figs. 4 to 13).

Figures captions

Figure 1. Geological context. (a) Simplified geological map of Northern South America. (b) Isopachs map of Phanerozoic sedimentary rocks (adapted from Exxon Production Research Company, 1994 and Cordani et al., 2016).

Figure 2. Regional cross-sections across northern South America (shown as thick blue lines labeled *a* to *c* on Fig. 1a). (a) Section from the Andes to the Foz do Amazonas basin along Solimões-Amazonas basin complex. (b) Section from the Andes to the Guiana-Suriname basin across the Guiana shield. (c) Section from the East Venezuela basin to the Potiguar basin across the Amazonas basin. Compiled after Crawford et al. (1985), Goes et al. (1990), Assine (1994), Talwani (2002), Watts et al. (2009), Hoorn et al. (2010), Wanderley-Filho et al. (2010) and Loparev et al. (2021).

Figure 3. (a) Explanation for the paleo-geological maps of Figures 4 to 13. Non-colored areas - including those obliquely striped in black - are domains of erosion or sedimentary bypass.

(b) Synthetic map showing selected localities and geological elements discussed in the text. Localities of the map are also shown on each paleomap of Figures 4 to 13 as open circles.

Figure 4. Geological reconstruction for the Late Permian (Guadalupian-Lopingian 270-250 Ma).

Figure 5. Geological reconstruction for the Triassic-Jurassic boundary (235-190 Ma).

Figure 6. Geological reconstruction for the Valanginian (140-133 Ma).

Figure 7. Geological reconstruction for the Aptian (120-115 Ma).

Figure 8. Geological reconstruction for the Albian (107-100 Ma).

Figure 9. Geological reconstruction for the Cenomanian (97-93 Ma).

Figure 10. Geological reconstruction for the Santonian (86-84 Ma).

Figure 11. Geological reconstruction for the Maastrichtian (72-66 Ma).

Figure 12. Geological reconstruction for the Middle Eocene (Lutetian-Bartonian 48-38 Ma).

Figure 13. Geological reconstruction for the Middle Miocene (Langhian-Serravallian 16-12 Ma).

Figure 14. The 3 successive regimes of the Northern South America source-to-sink systems. (a) Superswell regime (Jurassic-Barremian; 270-120 Ma; see Figs. 5 and 6) sustained by very long wavelength (x 1000 km) asthenospheric support under northwestern Gondwana. (b) Pre-Andean source-to-sink regime (Aptian-Santonian, 120-84 Ma; see Figs. 7-10). During that period, the transcontinental Amazonas-Solimões trough would has been intermittently closed by a continental divide in the vicinity of the Purus arch, such as during the Cenomanian (see Figs. 9 and 3b). (c) Andes-dominated source-to-sink regime (Maastrichtian to the present, 84-0 Ma; see Figs 11-13). That period saw (i) the formation and eastward growth of Andean retro-foreland basins, (ii) the eastward migration of the axial drainage of the Andean retro-foreland basin flowing to the northern coast of South America and (iii) the establishment of the modern transcontinental Amazon east-flowing drainage in the Amazonas-Solimões trough by the end of the Miocene. See text for further explanation.

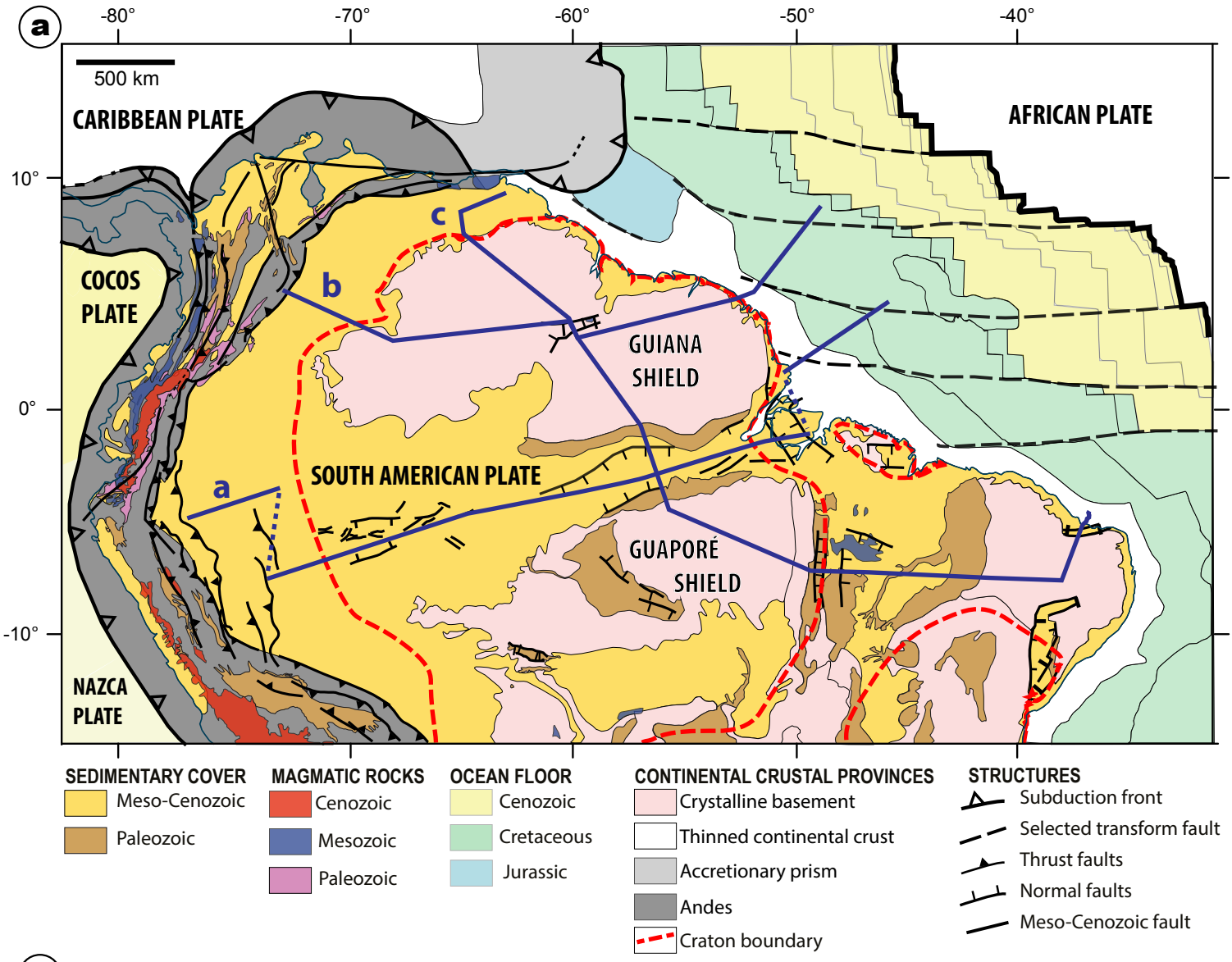

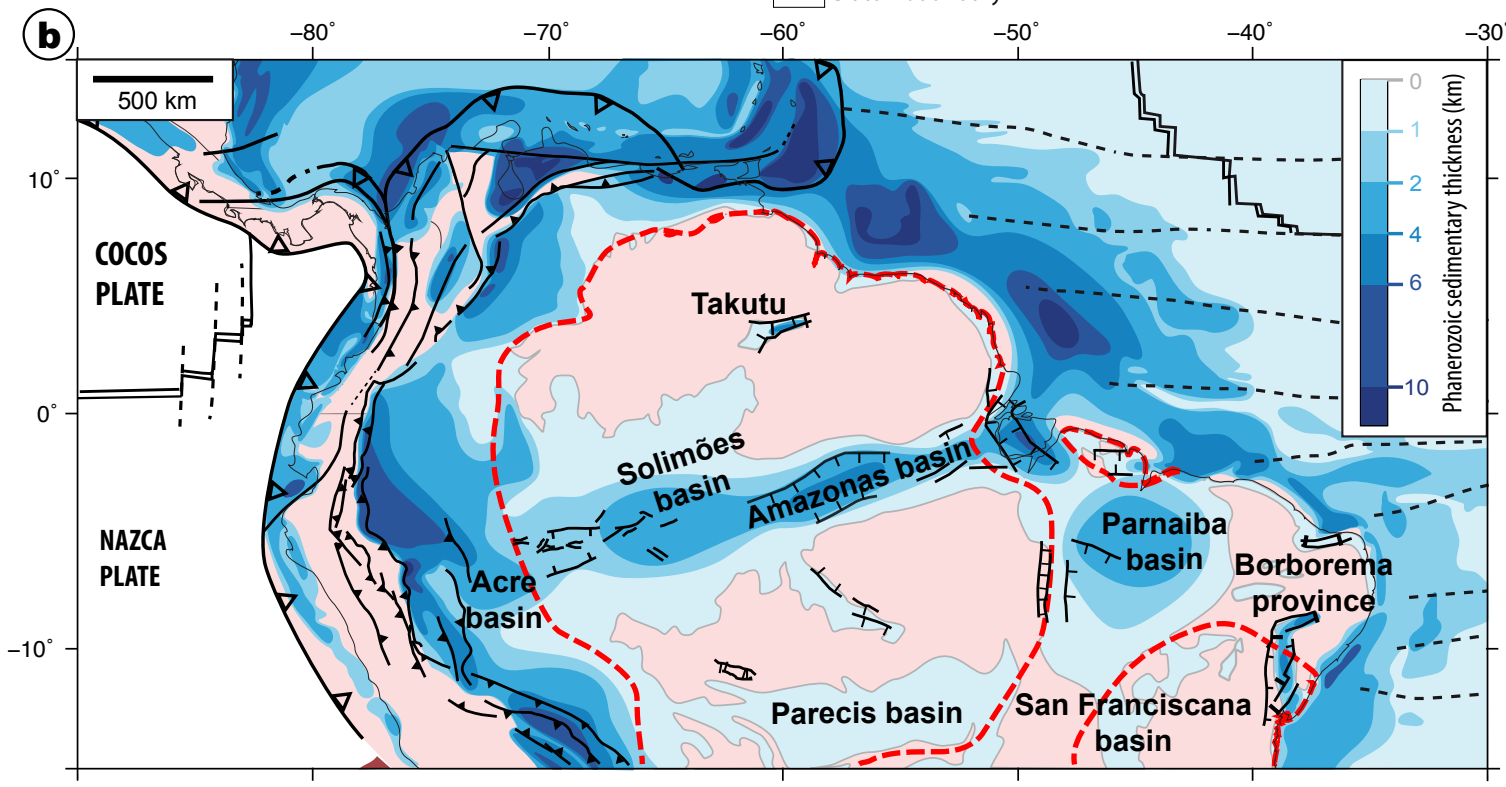

Bajolet et al., Figure 1

Figure 2

Click here to access/download;Figure;Fig2.CoupesRegionales.pdf

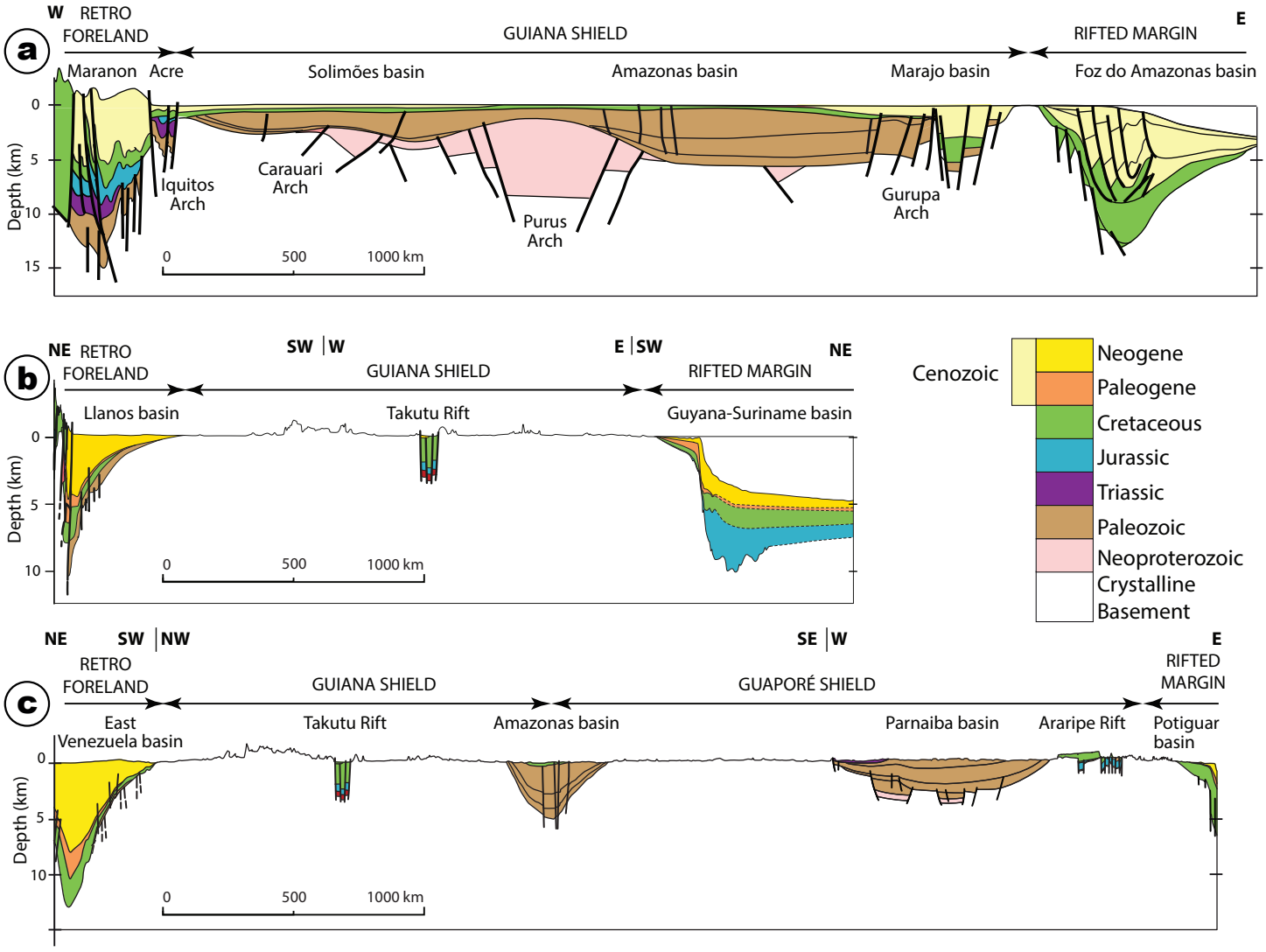

Bajolet et al., Figure 2

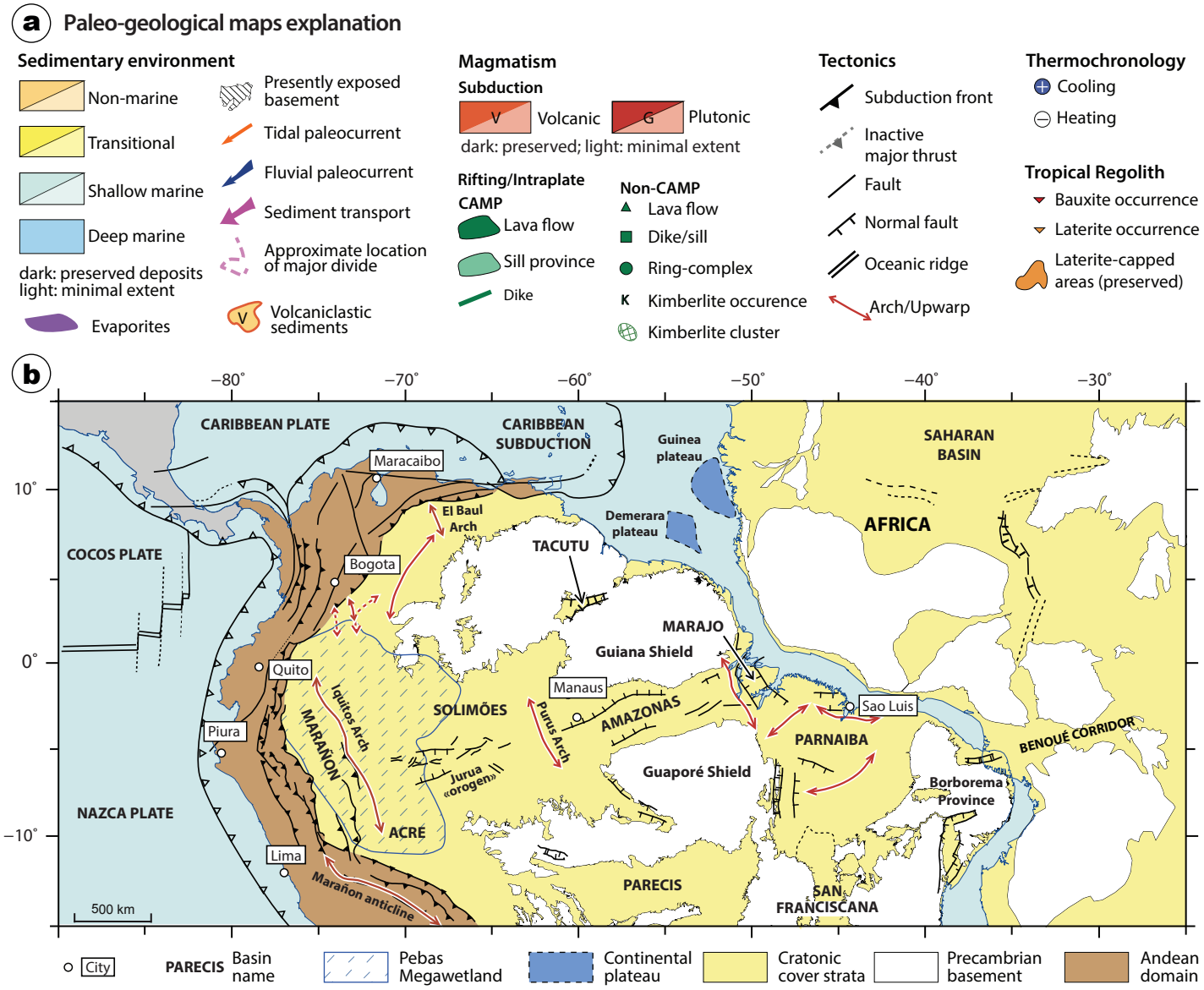

Bajolet et al., Figure 3

Figure 4

Click here to access/download;Figure;Fig4.pdf

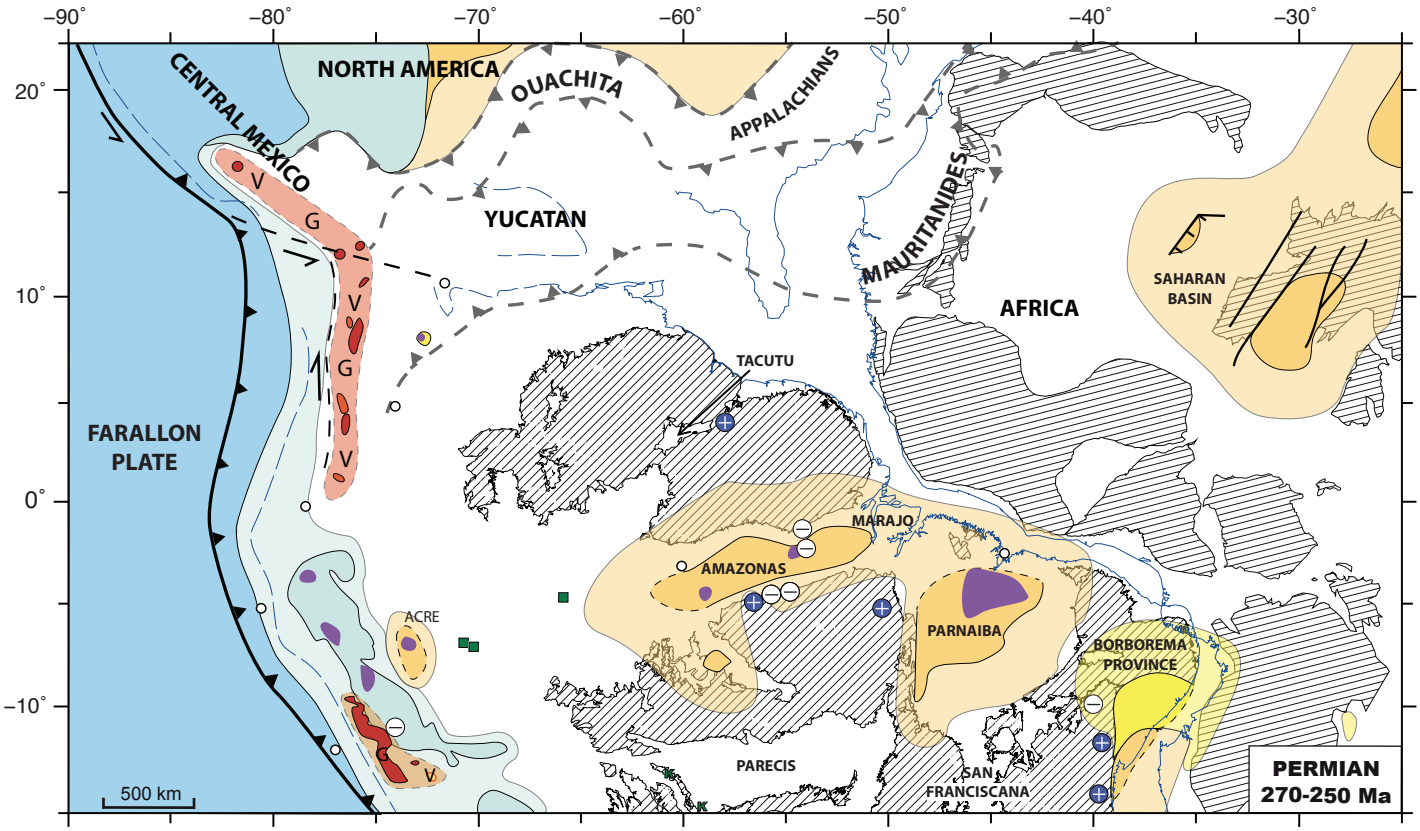

Bajolet et al., Figure 4

Figure 5

Click here to access/download;Figure;Fig5.pdf

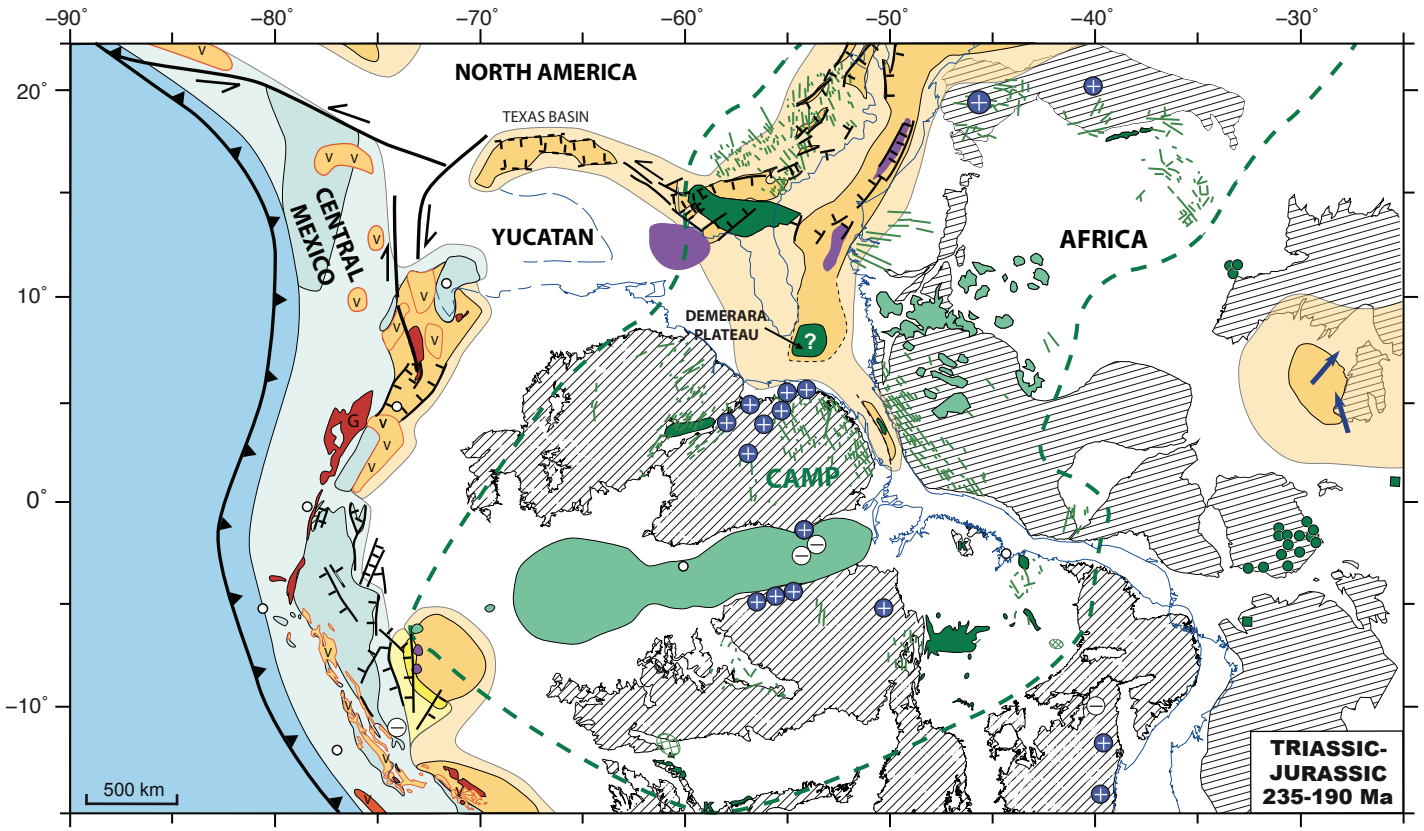

Bajolet et al., Figure 5

Figure 6

Click here to access/download;Figure;Fig6.pdf

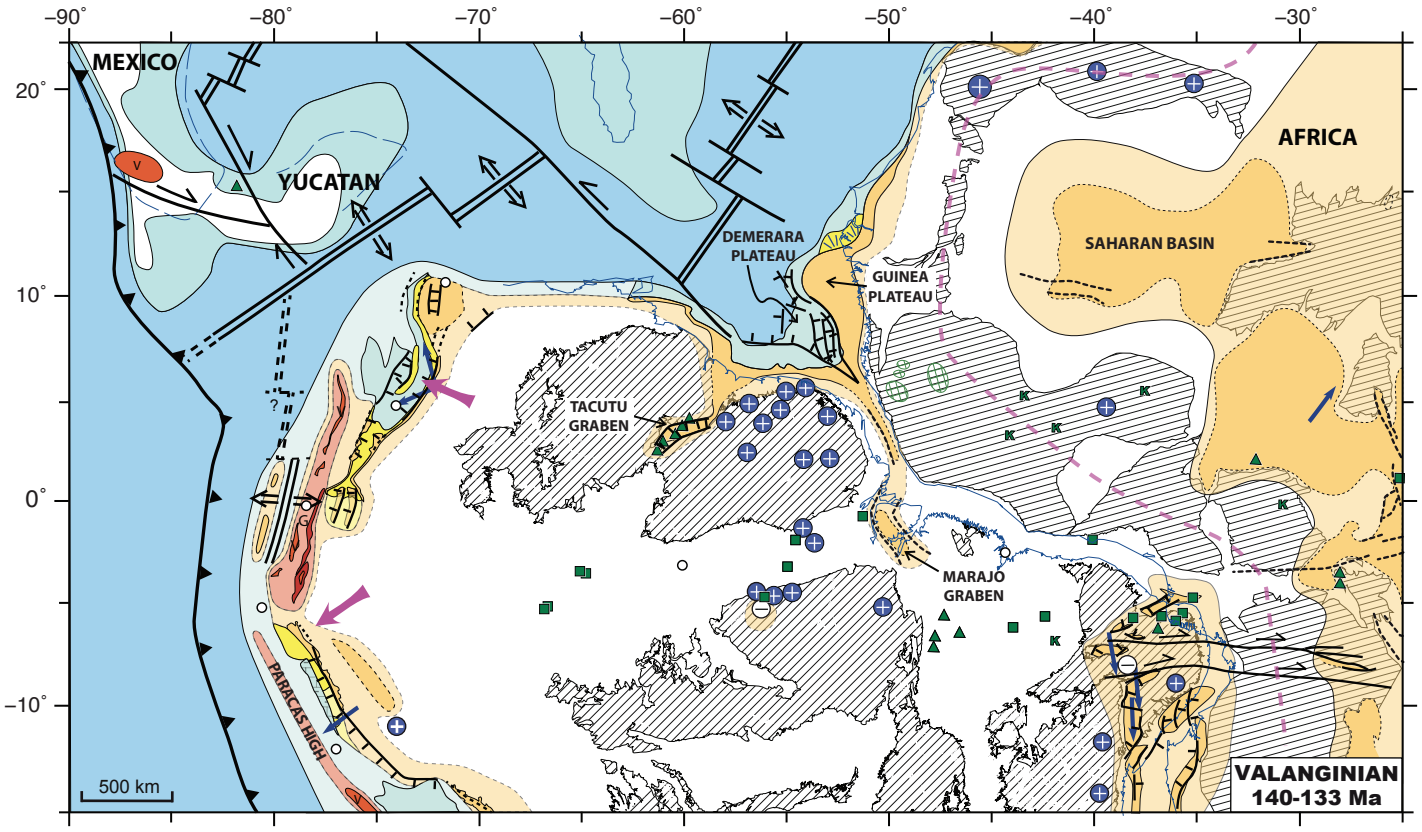

Bajolet et al., Figure 6

Figure 7

Click here to access/download;Figure;Fig7.pdf

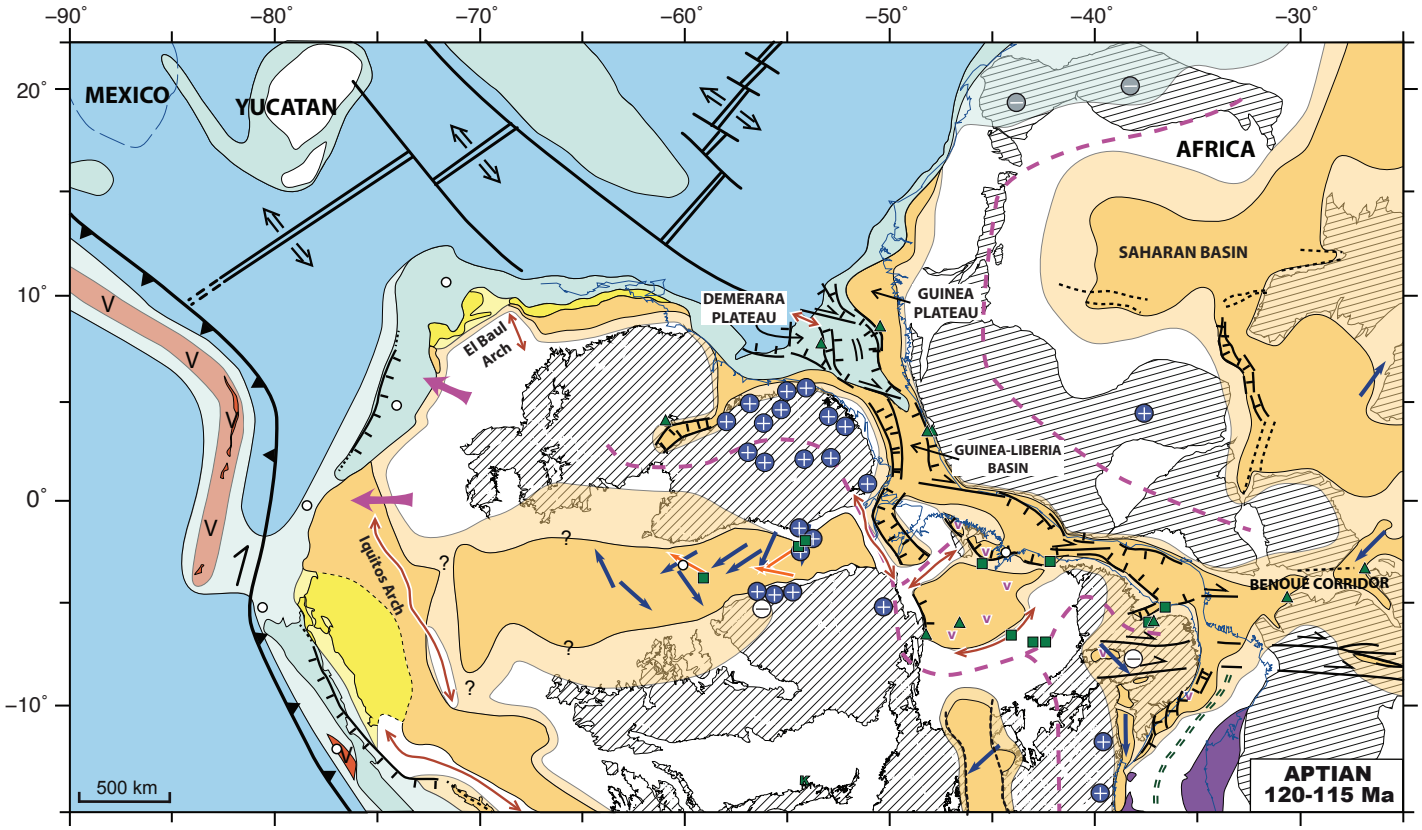

Bajolet et al., Figure 7

Figure 8

Click here to access/download;Figure;Fig8.pdf

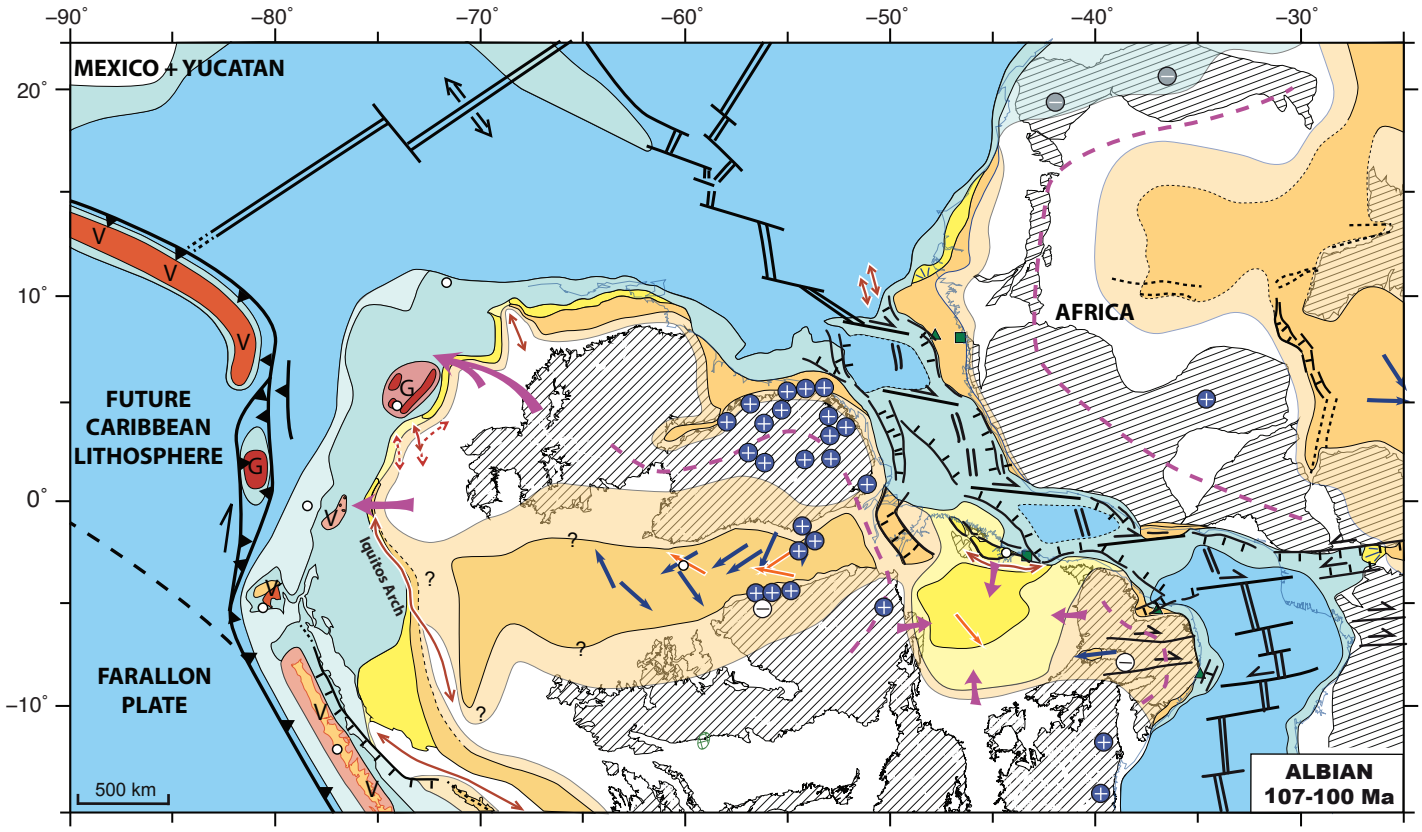

Bajolet et al., Figure 8

Figure 9

Click here to access/download;Figure;Fig9.pdf

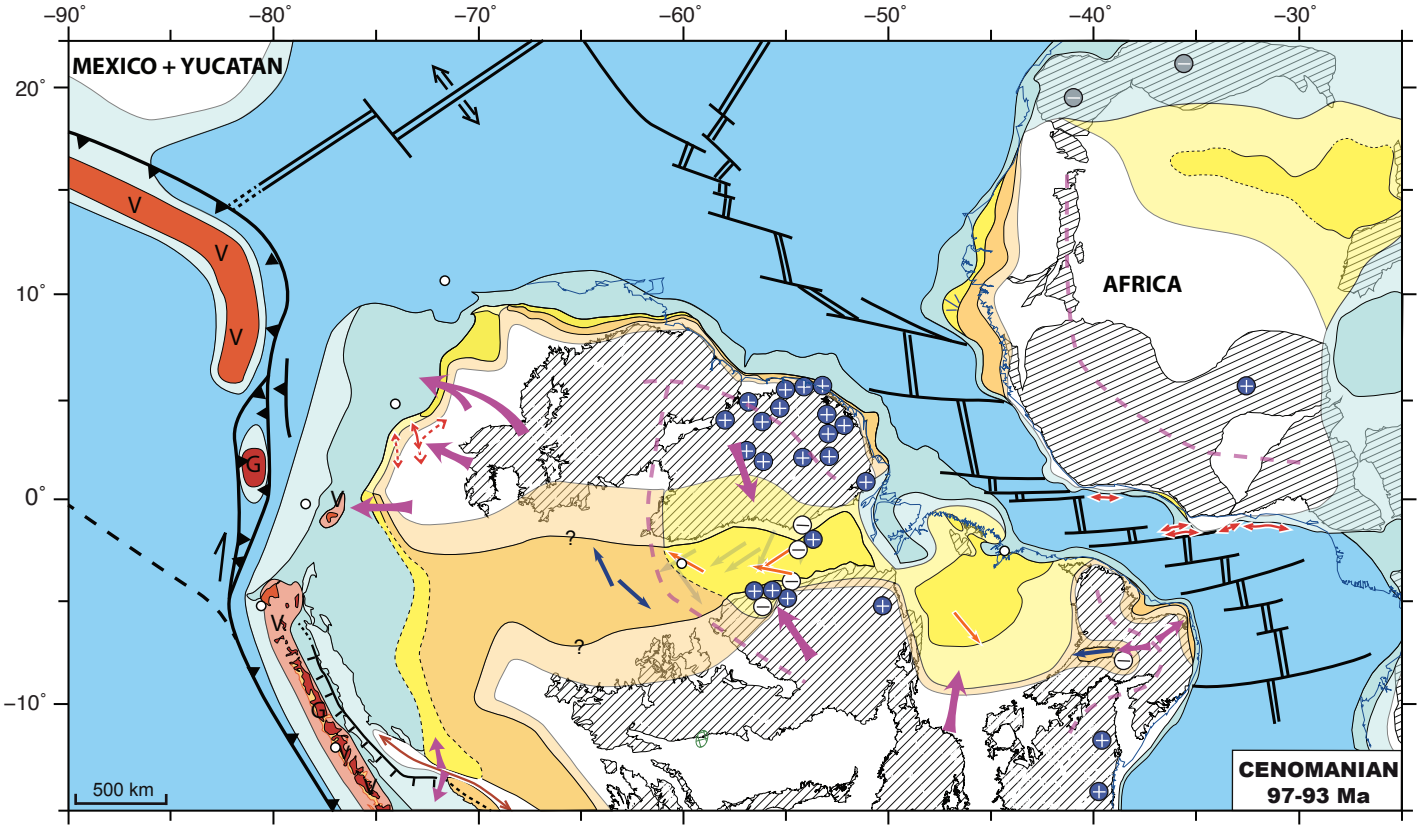

Bajolet et al., Figure 9

Figure 10

Click here to access/download;Figure;Fig10.pdf

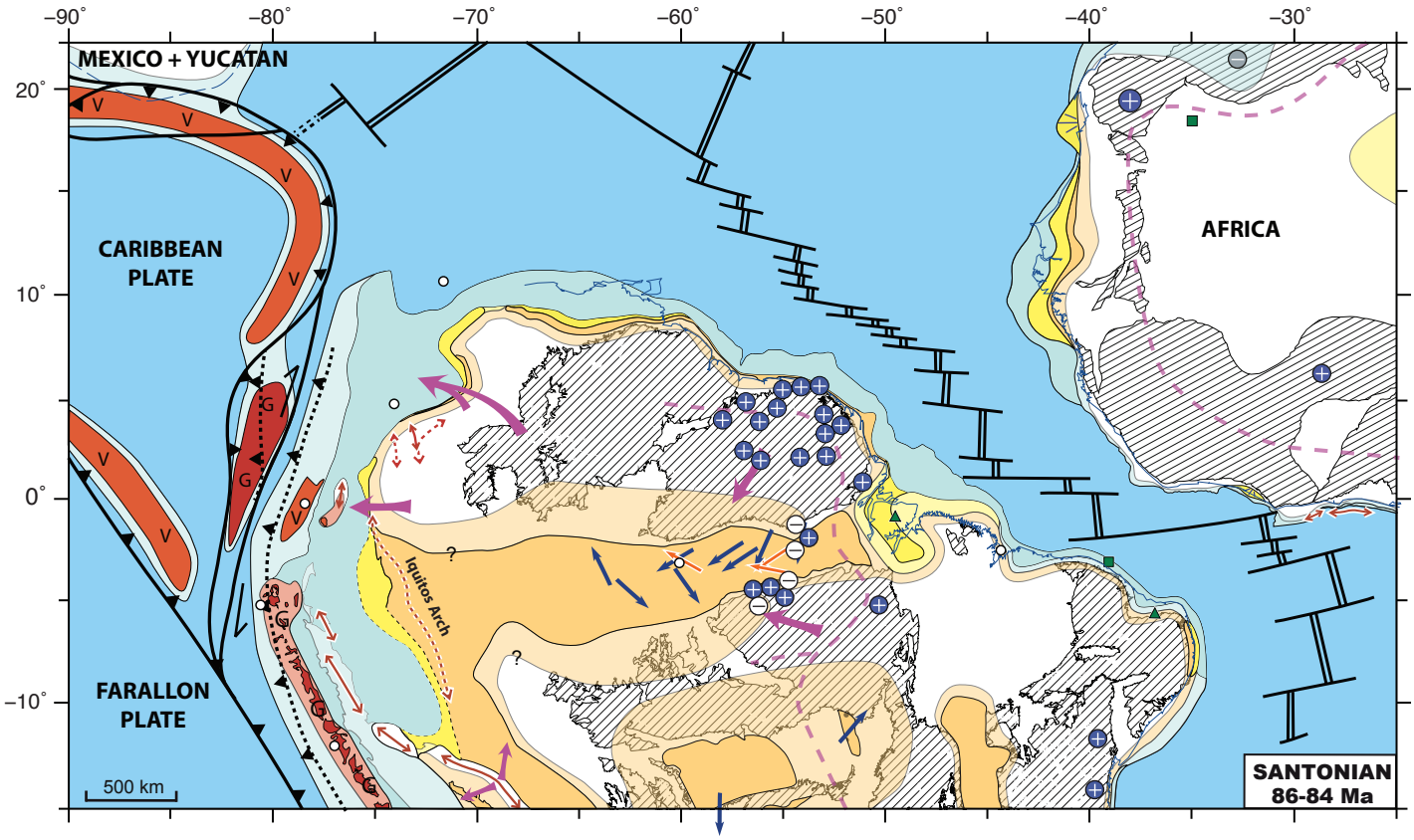

Bajolet et al., Figure 10

Figure 11

Click here to access/download;Figure;Fig11.pdf

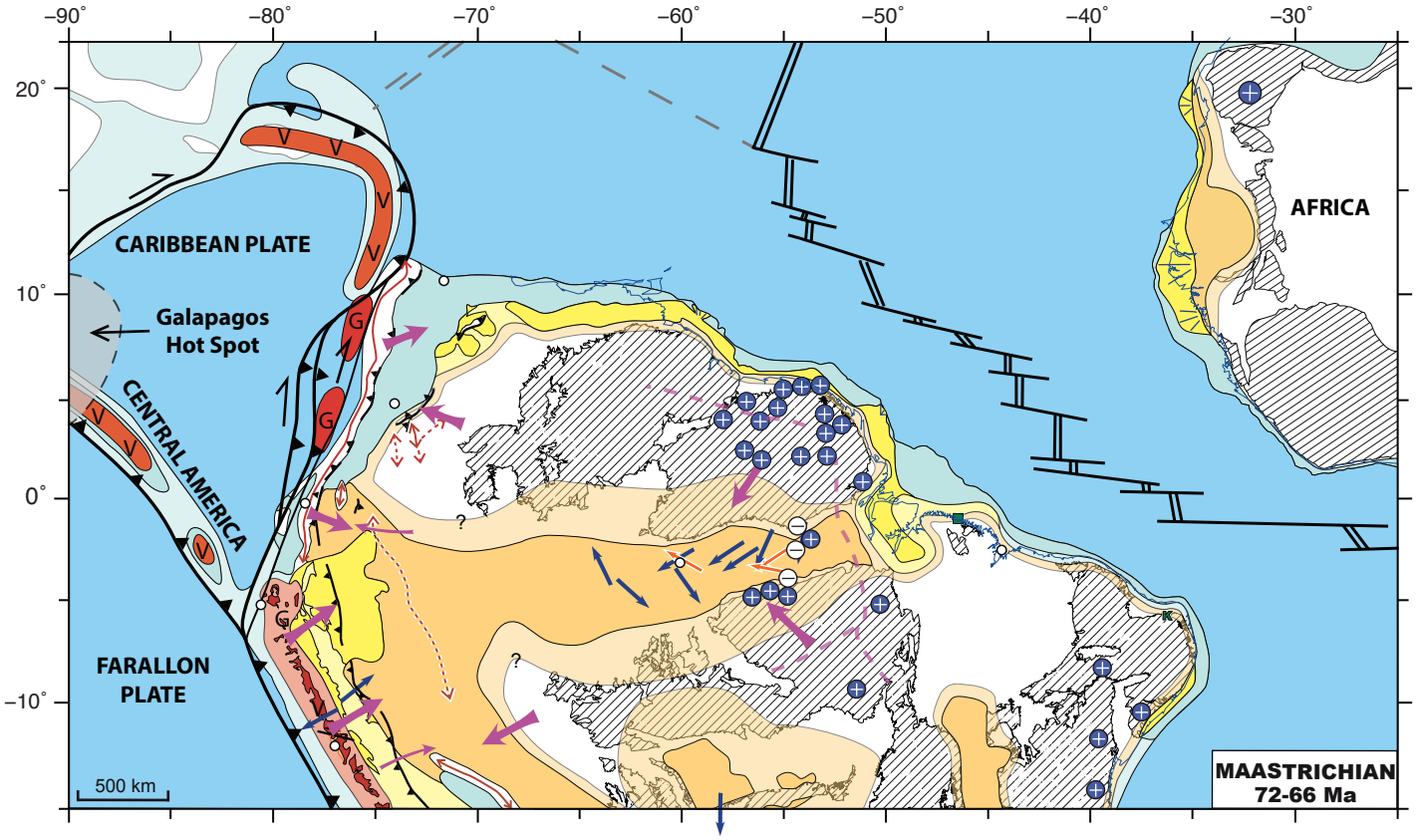

Bajolet et al., Figure 11

Figure 12

Click here to access/download;Figure;Fig12.pdf

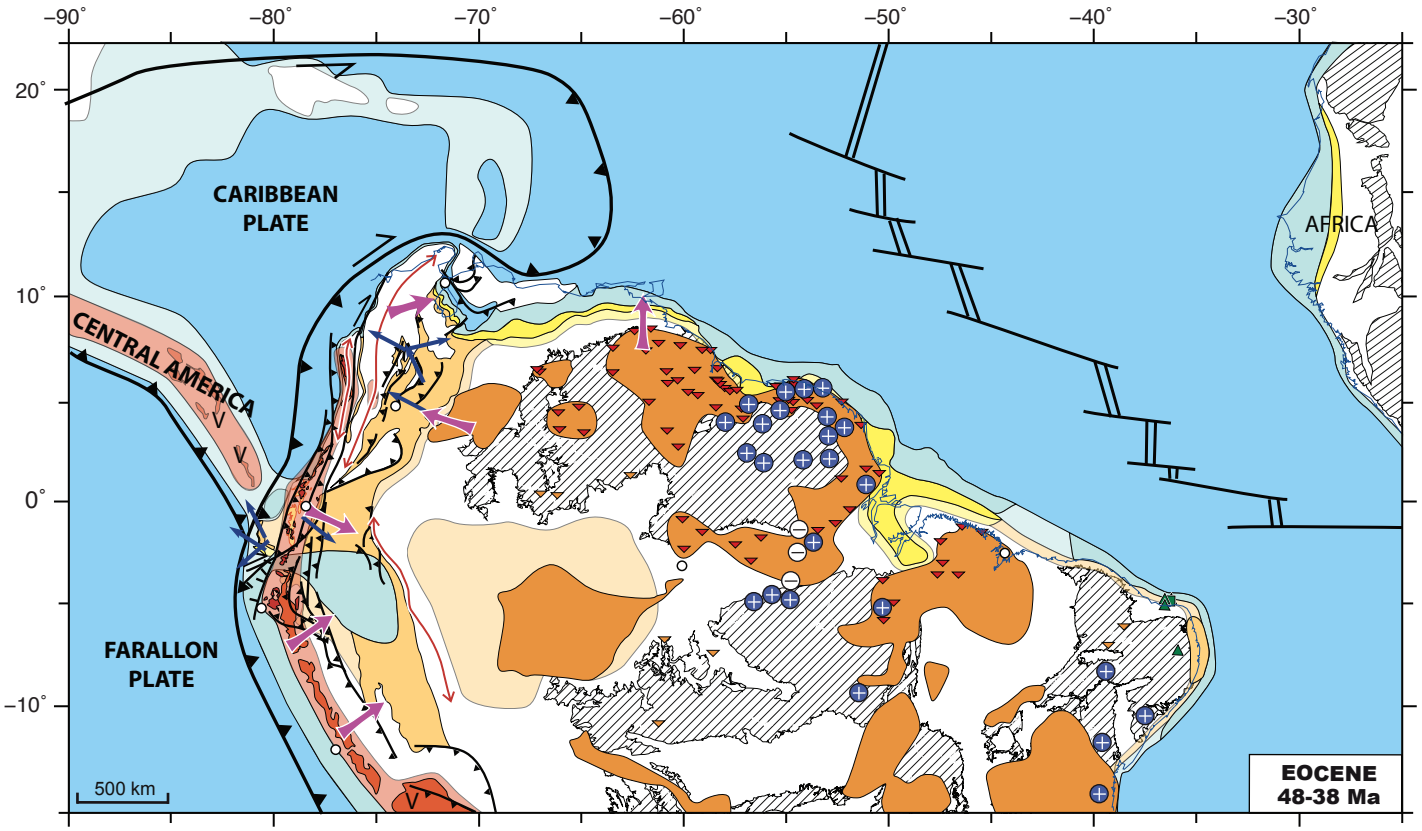

Bajolet et al., Figure 12

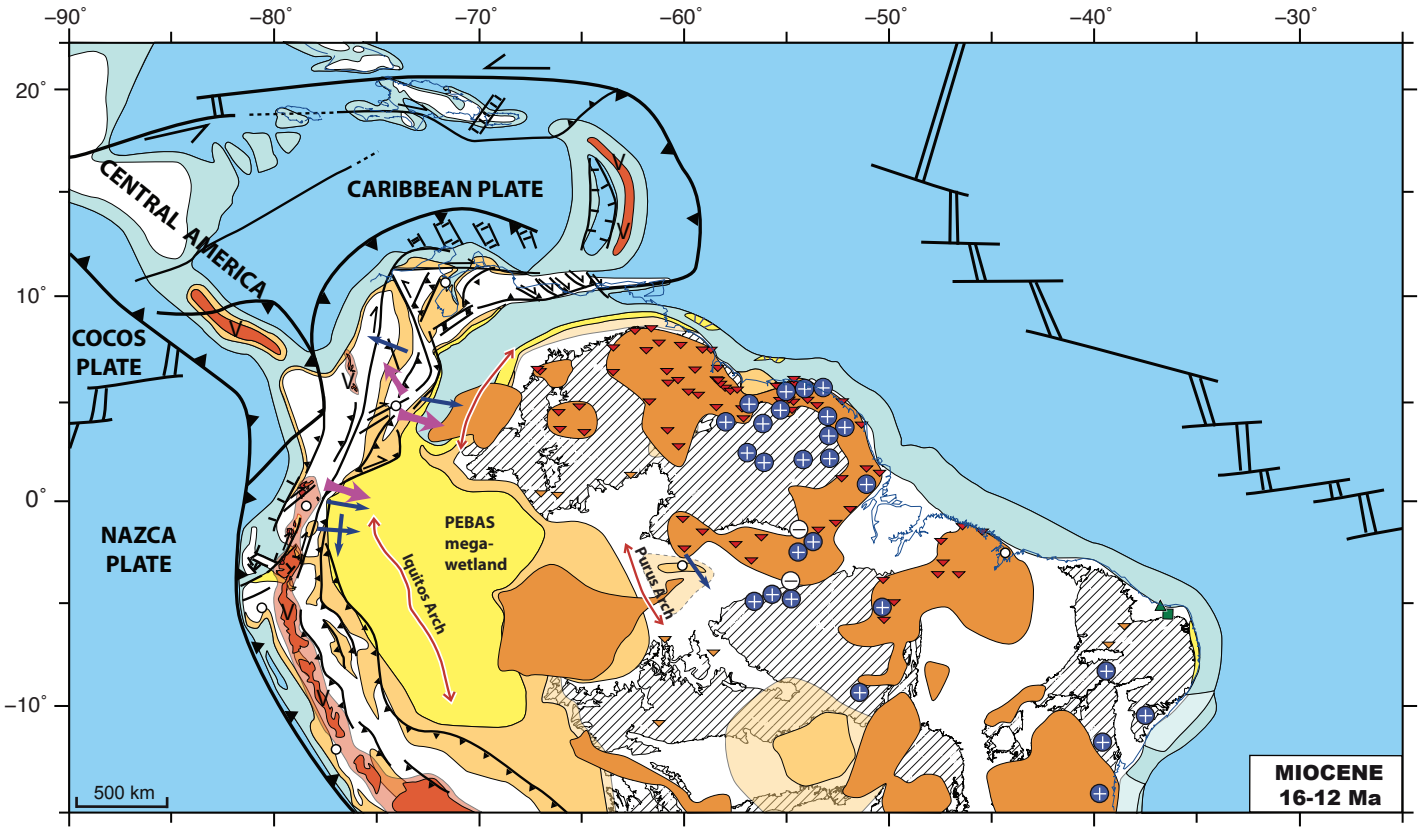

Bajolet et al., Figure 13

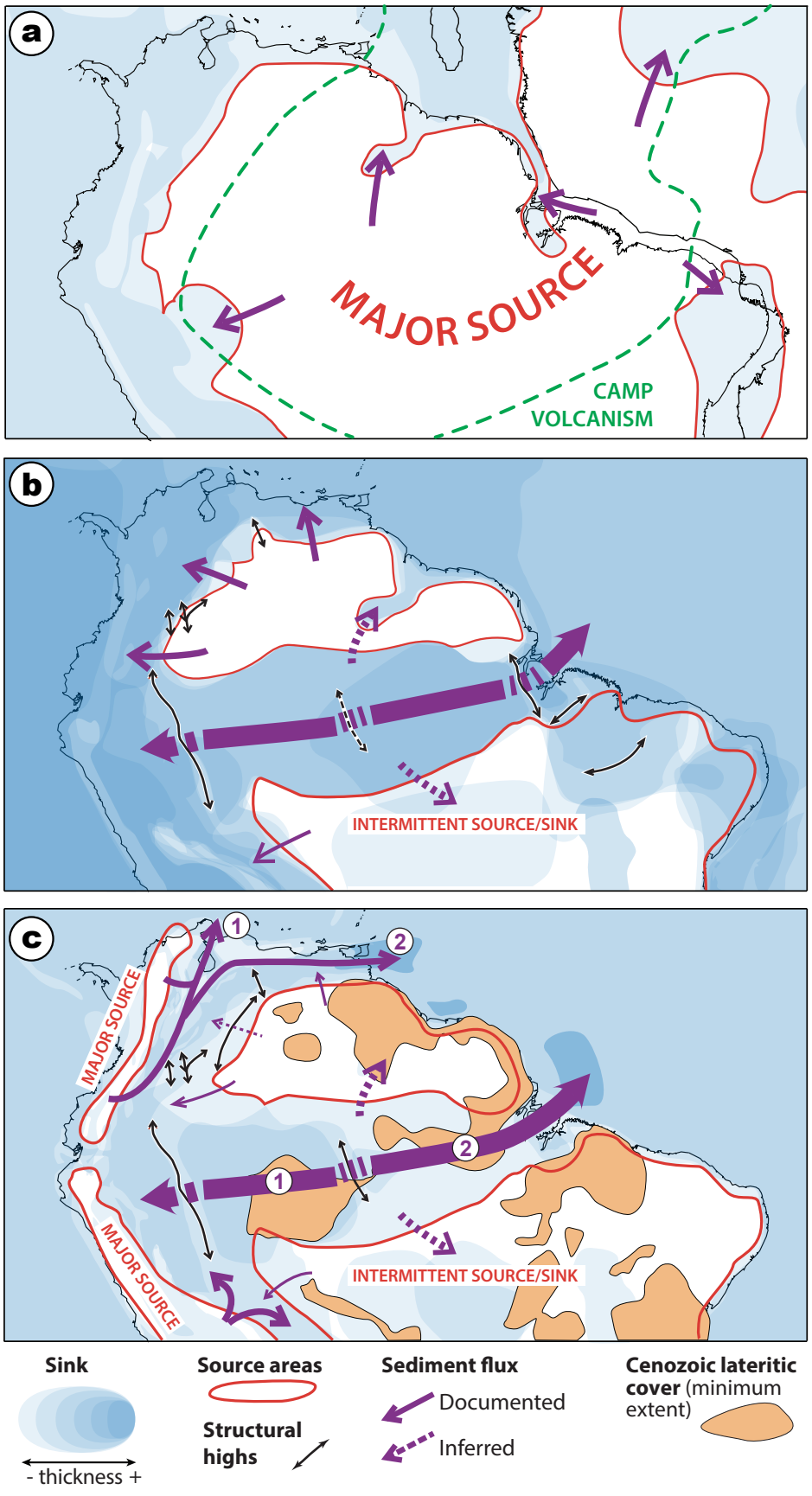

Superswell-dominated source-to-sink systems (Triassic - Barremian)

Pre-Andean source-to-sink systems (Aptian - Santonian)

Andes-dominated source-to-sink systems (Maastrichtian - Present)

Bajolet et al., Figure 14

Bajolet al., Table 1

		Paleogeographic maps									
THEMATIC GEOLOGICAL ITEMS	REFERENCES	270-250 Ma	235-190 Ma	140-133 Ma	120-115Ma	107-100Ma	97-93Ma	86-84 Ma	72-66 Ma	48-38 Ma	16-12 Ma
Sedimentary record											
Atlantic margin											
	Caixeta et al., 2007	X		X	X	X	X	X	X	X	X
	De Andrade Campos Neto et al., 2007	X		X	X	X	X	X	X	X	X
	Sapin et al., 2016		X	X	X	X	X	X	X	X	X
	Chaboureau et al., 2013			X	X						
	Figueiredo et al., 2007			X	X	X	X	X	X	X	X
	Zalán and Matsuda, 2007			X	X	X	X	X	X	X	X
	Gontijo et al., 2007			X	X	X	X	X	X	X	X
	Da Cruz Pessoa Neto et al., 2007			X	X	X	X	X	X	X	X
	Trosdtorf et al., 2007				X	X	X	X	X	X	X
	Condé et al., 2007				X	X	X	X	X	X	X
	Graddi et al., 2007				X	X	X	X	X	X	X
	Rangel et al., 2007				X	X	X	X	X	X	X
	Soares et al., 2007				X	X	X	X	X	X	X
	Córdoba et al., 2007				X	X	X	X	X	X	X
	Rossetti et al., 2013										X
	Ye et al., 2017 and references therein			X	X	X	X	X			
	Loparev et al., 2021		X	X	X	X	X	X	X	X	X
Caribbean margin/Central and North America											
	Soreghan and Soreghan, 2013	X									
	Foster et al., 2014	X									
	Sweet et al., 2013	X									
	Dickinson et al., 2010		X								
	Algar and Pindell, 1993			X	X	X	X	X	X	X	X
	Erlich and Barrett, 1992				X	X	X	X	X	X	X
	Parnaud et al., 1995				X	X	X	X	X	X	X
	Iturralde-Vinent, 2006				X				X		
	Arnaud et al., 2000				X	X					
	Mann et al., 2006									X	X
	Escalona and Mann, 2011										X

Intracontinental areas											
	Abrantes et al., 2016	X									
	Matsuda et al., 2004	X									
	da Cruz da Cunha et al., 2007a	X	X	X	X	X	X	X	X	X	X
	da Cruz da Cunha et al., 2007b	X	X	X	X	X	X	X	X	X	X
	Assine, 2007	X	X	X	X	X	X	X	X	X	X
	Vaz et al., 2007a	X	X	X	X	X	X	X	X	X	X
	Vaz et al., 2007b	X	X	X	X	X	X	X	X	X	X
	Silva et al., 2007	X	X	X	X	X	X	X	X	X	X
	Costa et al., 2007a	X	X	X	X	X	X	X	X	X	X
	Costa et al., 2007b	X	X	X	X	X	X	X	X	X	X
	Zalán and Silva, 2007	X	X	X	X	X	X	X	X	X	X
	Zalán, 2007	X	X	X	X	X	X	X	X	X	X
	Wanderley-Filho et al., 2007	X	X	X	X	X	X	X	X	X	X
	Crawford et al., 1985		X	X	X	X					
	Mosmann et al., 1986		X	X	X	X	X	X	X	X	X
	Scherer et al., 2014			X							
	Figueiredo et al., 2016			X	X						
	Valença et al., 2003			X	X	X					
	Assine, 1994			X	X	X	X				
	Varejão et al., 2016				X						
	Custódio et al., 2017				X						
	Scherer et al., 2015				X						
	Campos and Dardenne, 1997				X			X	X		
	Sgarbi, 2000				X			X	X		
	Dino et al., 1999				X	X	X	X	X		
	Mendes, 2013				X	X	X	X	X	X	X
	Mendes et al., 2012										
	Rossetti and Netto, 2006						X				
	Bahia et al., 2006							X	X		
	Rubert et al., 2017							X	X		X
	Abinader, 2008									X	
	Antoine et al., 2013										X
Foreland basins											
	Mathalone and Montoya, 1995	X	X								
	Gonçalves et al., 2002		X	X	X	X	X	X	X	X	X
	Bayona et al., 2008			X	X	X	X	X	X	X	X
	Macellari, 1988			X	X	X	X	X	X		

	Moreno-Lopez and Escalona, 2015			X	X	X	X	X	X		
	Balkwill et al., 1995			X	X	X	X	X	X		
	Cooper et al., 1995			X	X	X	X	X	X		X
	Espurt et al., 2008				X	X	X	X	X	X	X
	Martinez et al., 1999				X	X	X	X	X		
	Sanchez et al., 1999				X	X	X	X	X		
	Dashwood and Abbotts, 1990				X	X	X	X	X		
	Louterbach et al., 2014									X	
	Reyes-Harker et al., 2015									X	X
	Hermoza et al., 2005									X	X
	Antoine et al., 2013										X
Andes											
	Laya and Tucker, 2012	X									
	Mathalone and Montoya, 1995	X	X								
	Sempere, 1995	X	X	X	X	X	X	X	X	X	X
	Rosas et al., 2007		X								
	Sempere et al., 2002		X								
	Jaillard et al., 1990		X								
	Macellari, 1988			X	X	X	X	X	X		
	Scherrenberg et al., 2012			X	X	X	X	X	X		
	Winter et al., 2010					X					
	Jaillard et al., 2005							X	X		
	Villamil, 1999								X	X	
	Parra et al., 2009								X	X	X
	Jaillard et al., 1995									X	
	Pindell and Tabbutt, 1995									X	X
	Nie et al., 2012									X	X
	Hungerbühler et al., 2002										X
Africa											
	Ye et al., 2017 and references therein		X	X	X	X	X	X	X	X	
	Linol et al., 2015c	X									
Plate boundaries and kinematic reconstructions											

	Elías-Herrera and Ortega-Gutierrez, 2002	X									
	Soreghan and Soreghan, 2013	X									
	Weber et al., 2007	X	X								
	Pindell and Kennan, 2009		X	X		X	X	X	X		
	Dickinson and Lawton, 2001		X	X							
	Matthews et al., 2016			X	X	X	X	X	X	X	X
	Moulin et al., 2010			X	X	X	X	X	X		
	Montes et al., 2019								X	X	X
	Escalona and Mann, 2011									X	X
Fault pattern and kinematics											
Atlantic margin											
	Ye et al., 2017 and references therein			X	X						
Intracontinental areas											
	Ye et al., 2017 and references therein		X	X	X	X	X	X	X		
	De Castro et al., 2008			X							
	Crawford et al., 1985			X	X						
	Valença et al., 2003			X	X	X					
	Reis et al., 2017				X						
Caribbean margin/Central and North America											
	Soreghan and Soreghan, 2013	X									
	Bartok, 1993	X									
	Weber et al., 2007	X									
	Dickinson and Lawton, 2001		X								
	Dickinson et al., 2010		X								
	MacRae and Watkins, 1995		X								
	Algar and Pindell, 1993									X	X
	Escalona and Mann, 2011										X
Andes											
	Pfiffner and Gonzales, 2013	X	X	X	X	X	X	X	X	X	X
	Sarmiento-Rojas et al., 2006		X	X	X						
	Aspden and Litherland, 1992		X	X	X						
	Scherrenberg et al., 2012, 2014			X	X	X	X	X	X		

	Pindell and Kennan, 2009								X	X	X
	Montes et al., 2019								X	X	X
	Jaillard et al., 2009								X	X	X
	Villamil, 1999								X	X	
	Hungerbühler et al., 2002										X
Foreland basins											
	Mathalone and Montoya, 1995		X								
	Balkwill et al., 1995			X							
	Bayona et al., 2008			X	X	X	X	X	X	X	X
	Moreno-Lopez and Escalona, 2015			X	X	X	X	X	X		
	Delgado et al., 2012										X
Africa											
	Ye et al., 2017 and references therein		X	X	X	X	X	X	X	X	
Magmatism											
Atlantic margin											
	Mizusaki et al., 2002	X	X	X	X	X	X	X	X	X	X
Intracontinental areas											
	Tappe et al., 2018	X	X	X			X				
	Mizusaki et al., 2002	X	X	X	X	X	X	X	X	X	X
	De Min et al., 2003		X								
	Hunt et al., 2009		X								
	Masun and Smith, 2008		X								
	Merle et al., 2011		X								
	Wanderley-Filho et al., 2005		X								
	Bulanova et al., 2010						X				
	Silveira, 2006								X		
Foreland basins											
	Barragan et al., 2005					X	X	X			
Andes											
	Boekhout et al., 2018	X									
	Mišković et al., 2009	X									
	Spikings et al., 2016	X									

	Van der Lelij et al., 2016a	X	X								
	Van der Lelij et al., 2016b	X	X								
	Jaillard et al., 1990		X								
	Spikings et al., 2015		X	X	X						
	Winter et al., 2010					X	X	X	X	X	
	Atherton and Webb, 1989					X	X	X	X	X	X
	Egüez et al., 2017									X	X
	Schütte et al., 2010									X	X
	Pindell and Tabbutt, 1995										X
Caribbean/Mexico											
	Centeno-García, 2017	X									
	Torres et al., 1999	X									
Africa											
	Ye et al., 2017 and references therein		X	X	X	X	X	X			
Thermochronology											
	Harman et al., 1998	X	X	X	X	X	X	X	X	X	X
	Jelinek et al., 2014			X	X	X	X	X	X	X	X
Sources and provenances											
	Horton et al., 2010		X	X	X	X	X	X	X	X	X
	Horton, 2018		X	X	X	X	X	X	X	X	X
	Moreno et al., 2020		X	X	X	X	X	X	X	X	
	Figueiredo et al., 2016			X	X						
	Saylor et al., 2011			X	X	X	X	X	X	X	
	Dantas et al., 2014				X	X	X	X	X		
	Mendes et al., 2015				X	X	X	X	X		
	Mapes et al., 2007				X	X	X	X	X		X
	Ruiz et al., 2004				X	X	X	X	X	X	X
	Martin-Gombojav and Winkler, 2008				X	X	X	X	X	X	X
	Nascimento et al., 2007					X					
	Gutierrez et al., 2019					X	X	X	X	X	X
	Silva et al., 2013						X	X	X	X	X

	Louterbach et al., 2018								X		
	Vallejo et al., 2017								X		
	Nie et al., 2012									X	X
	Caballero et al., 2013									X	X
	Roddaz et al., 2005, 2006, 2012										X
	George et al., 2019										X

Figure S1